Diffusion, attraction and collapse

Michael P. Brenner†, Peter Constantin‡, Leo P. Kadanoff‡, Alain Schenkel‡ and Shankar C. Venkataramani‡§

† Department of Mathematics, Massachusetts Institute of Technology, Cambridge, MA 02139, USA

‡ Department of Mathematics, University of Chicago, 5734 University Ave., Chicago, IL 60637, USA

Abstract.

We study a parabolic-elliptic system of partial differential equations that arises in modeling the overdamped gravitational interaction of a cloud of particles or modeling chemotaxis in bacteria. The system has a rich dynamics and the possible behaviors of the solutions include convergence to time independent solutions and the formation of finite-time singularities. Our goal is to describe the different kinds of solutions that lead to these outcomes. We restrict our attention to radial solutions and find that the behavior of the system depends strongly on the space dimension d. For $2 < d < 10$ there are two stable blowup modalities (self-similar and Burgers-like) and one stable steady state. On unbounded domains, there exists a one-parameter family of unstable steady solutions and a countable number of unstable blowup behaviors. We document connections between one unstable blowup behavior and both a stable steady state and a stable blowup, as well as connections between one unstable blowup and two different stable blowups. There is a topological and stability correspondence between the various asymptotic behaviors and this suggests the possibility of constructing a global phase portrait for the system that treats the global in time solutions and the blowing up solutions on an equal footing.

AMS classification scheme numbers: 35K55,35B05,58G11,58G40

Submitted to: *Nonlinearity*

§ Corresponding author: `shankar@math.uchicago.edu`

1. Introduction

In this paper we will consider solutions of the parabolic-elliptic system

$$\begin{aligned} \partial_t \rho &= \Delta\rho - \nabla\cdot(\rho\nabla c) \\ -\Delta c &= \rho. \end{aligned} \tag{1}$$

The scalar functions $\rho = \rho(\mathbf{x}, t)$ and $c = c(\mathbf{x}, t)$ depend on $\mathbf{x} \in \Omega \subseteq \mathbf{R}^d$ and on $t \geq 0$. We are interested in solving the system (1) for domains Ω that are bounded as well as when $\Omega = \mathbf{R}^d$ ("the unbounded case"). For the solutions on a bounded domain, the boundary conditions are zero flux of the scalar ρ through $\partial\Omega$ and the scalar c is zero on $\partial\Omega$. For solutions on $\mathbf{R}^d$, the boundary conditions are decay at infinity in ρ and in c. These equations constitute a simplification of the Keller-Segel model [1] that was introduced in the context of chemotactic aggregation. In this interpretation, ρ represents the density of the bacteria and c represents the density of the chemo-attractant. These equations can also be interpreted as an overdamped version of the Chandrasekhar equation for the gravitational equilibrium of isothermal stars [2] or with the evolution of self interacting clusters of particles in a viscous regime where ρ is the mass density and c is the gravitational potential (See [3, 4] and references therein).

Suppose one starts with some initial density distribution and asks: what is the final state of the system? Figures 1, 2 and 3 show numerical simulations that give three different final fates: In Fig. 1, the diffusion wins and the density ρ spreads out so that the system heads for a steady state. In Fig. 2, the density ρ blows up at some finite time T. En route to the blowup, the maximum of the $\rho(r, t)$ is always at the origin. In Fig. 3, the density ρ again blows up at a finite time T, but, in this case, the solution corresponds to an imploding shock and prior to the blowup, the location of the maximum of $\rho(r, t)$ is always off the origin. We wish to study these and the other possible dynamical outcomes.

The problem has several experimental realizations. As was discussed above, the equations represent the dissipative dynamics of a mass density ρ interacting with itself via the gravitational potential. In this example blowup corresponds to gravitational collapse at low Reynolds numbers. The time dynamics of gravitational collapse into black holes is a topic of current interest [5]. Another realization occurs in bacterial chemotaxis – the bacteria drift up the gradient of the attractant c. This last example has recently been realized with *E. Coli* [6, 7]. In this context, blowup corresponds to the formation of dense aggregates of bacteria. The experiments show a competition between cylindrically symmetric collapse (in which the final state is a line) and spherically symmetric clumping to a geometrical point.

From the mathematical side, the problem is one of a class of blowup problems [8] in which small scales are produced in a finite time. An equation with finite time blowup that has been the subject of much study is the nonlinear Schrödinger equation [9]. The blowup in the system (1) bears some similarities to the blowup in the nonlinear Schrödinger equation, both in the scaling of the self-similar blowing up solutions and in

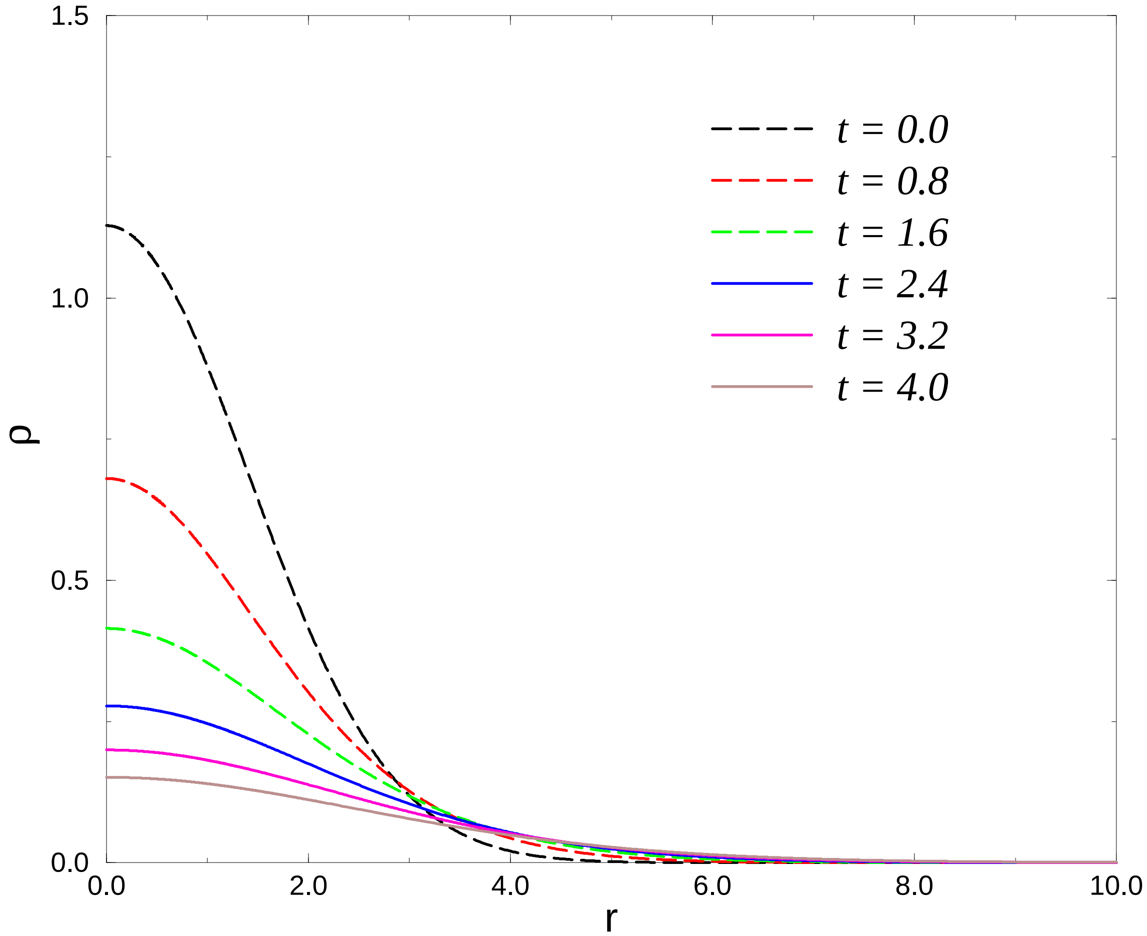

Figure 1. Simulation with spherically symmetric initial data in three dimensions. The solution goes to a time independent density profile for large times

the dependence of the blowup on the dimensionality of the space. A canonical example for finite time blowup in a parabolic PDE is the finite time blowup in the solutions of the semi-linear heat equation

$$\partial_t \rho = \Delta\rho + \rho^2.$$

This problem has been studied extensively by many authors (See [10], [11], [12], [13] and references therein.) All the possible blowup profiles for this equation have been classified [12] and recent work [13] significantly extends the scope of the analysis. The equation for the density ρ in (1) can be rewritten as

$$\partial_t \rho = \Delta\rho - \nabla c \cdot \nabla\rho + \rho^2,$$

so that these equations are similar to the semi-linear heat equations except for the presence of the advection term $\nabla c \cdot \nabla\rho$. It turns out that the presence of this term changes significantly the properties of the solutions. Unlike the semi-linear heat equation, the mechanism for the blowup in the system (1) depends on the space

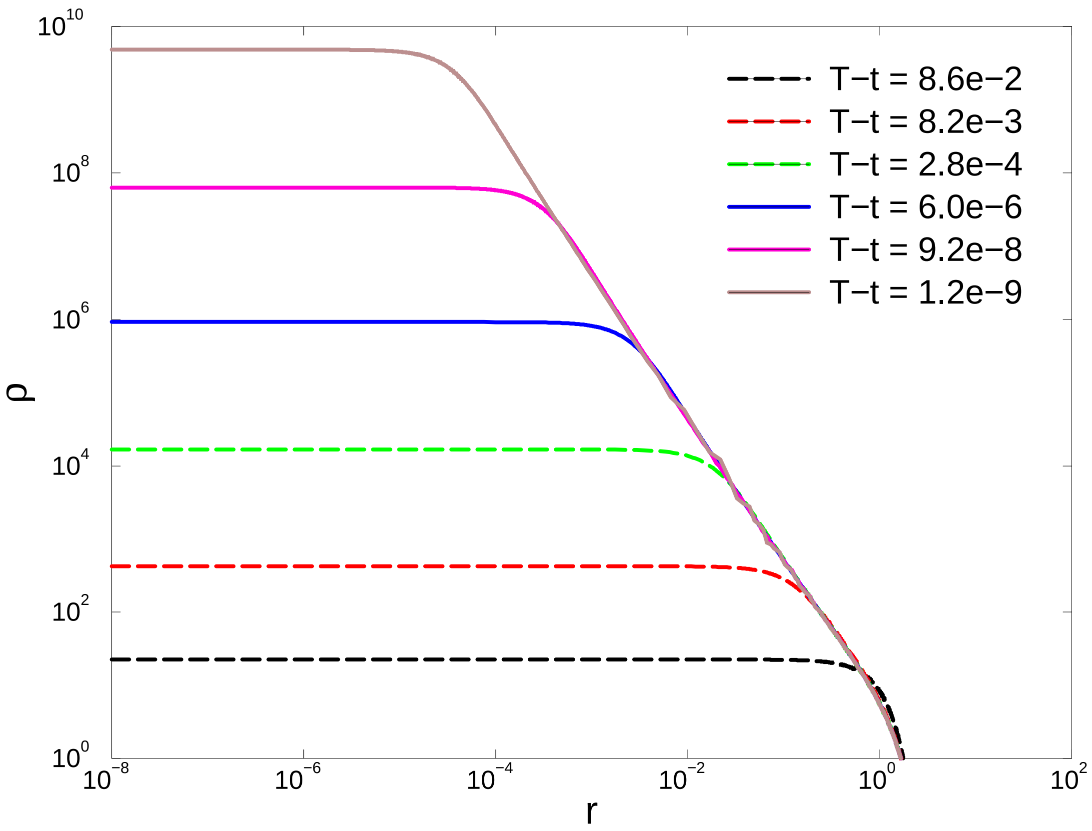

Figure 2. Simulation with spherically symmetric initial data in 3 dimensions. The figure shows a double log plot of blowup at the origin at a finite time T. The maximum density increases rapidly with time signaling the onset of a singularity.

dimension d. In the semi-linear heat equation blowup is self-similar; for the system in (1), in addition to one stable and many unstable self-similar blowup profiles, there exists another, stable, qualitatively different blowup modality: a collapsing Burgers-like shock [14] (See Figure 3.) The system is rich: two different stable blowup regimes and countable many unstable ones coexist with stable and unstable steady states.

Blowup of solutions of the Keller-Segel equations was predicted by Nanjudiah [15] and analyzed in a definitive paper of Childress and Percus [16]. The question of blowup in the Keller-Segel equations and the closely related problem of blowup in the system (1) has been studied by many authors (See [14], [17]-[26] and references therein). In this paper, we restrict ourselves to the investigation of radial solutions of the system (1) in $\mathbf{R}^d$ as well as bounded spherical domains in $\mathbf{R}^d$ for $d > 2$. It is known that $d = 2$ is the critical dimension for this system, that is finite time singularities in the solutions of (1) can occur for $d \geq 2$ but all the solutions are regular for $d = 1$ [20].

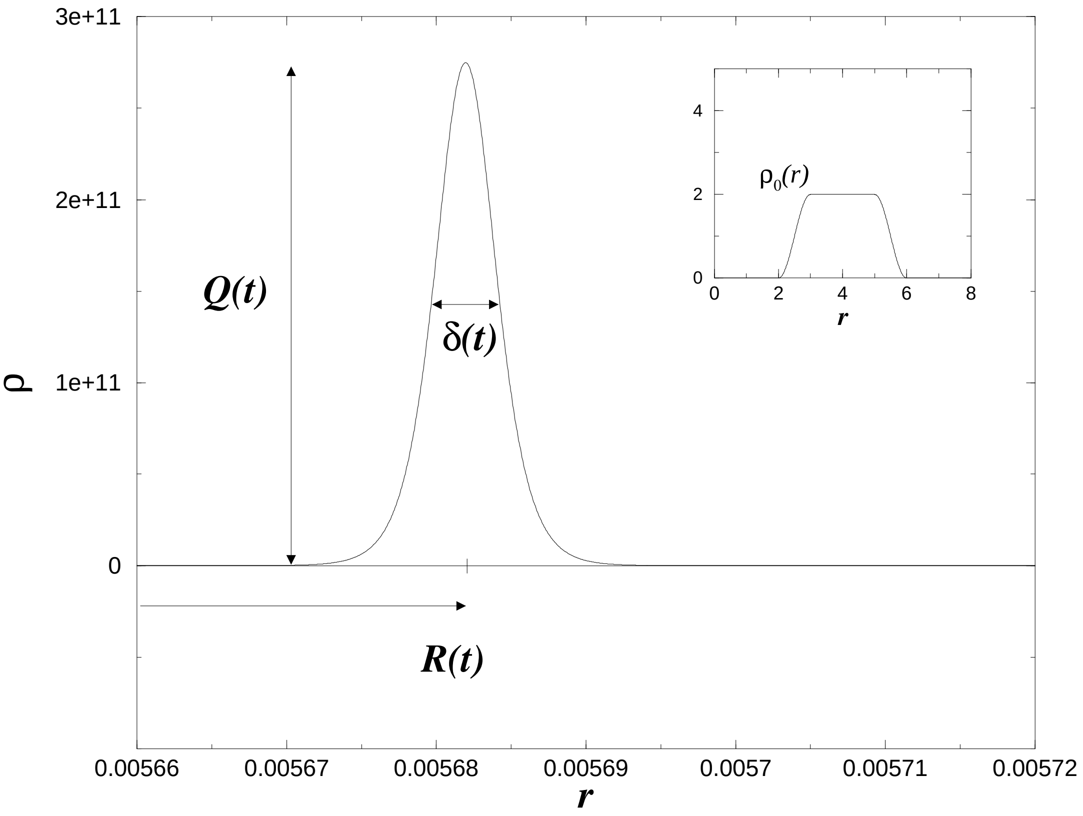

Figure 3. The density profile with spherically symmetric initial data in 3 dimensions at time to blowup $T - t = 7.13 \times 10^{-9}$ for the initial condition shown in the upper right corner.

The goal of this paper is to understand the different kinds of (radial) solutions of the system (1). It is well-known that a *dissipative* system (a dynamical system with a closed an bounded absorbing set) with a Lyapunov functional, has solutions that exist for all time, and the dynamical behavior is characterized by a global attractor that is formed by the steady solutions and their unstable manifolds [27, 28]. The existence of a Lyapunov functional rules out the possibility of periodic or chaotic solutions. Knowing all the steady solutions and their respective stabilities will enable the construction of a global phases portrait for the system that will describe the qualitative features of all the solutions (trajectories) of the system.

The system in (1) has an energy functional (See also [24, 25, 26]) that is non-increasing on solutions. Unlike the dynamical systems mentioned above, this system is not dissipative; moreover it has both global (in time) solutions, and solutions with finite time singularities. We will present evidence that it might still be possible to construct a global phase portrait of the system, and in this phase portrait the singular behavior (blowup) and the non-singular behavior (convergence to steady states) are treated on an equal footing. To study the question of whether it is indeed possible to construct a global phase portrait, we will analyze the various solutions for this system and their stability.

1.1. Summary of results

In this paper, we restrict ourselves to the analysis of radial solutions. For radial solutions, it is useful to define a quantity $h(r,t)$ (also see Eqs. (7) and (11) below) by

$$h(r,t) = \frac{1}{2r^{d-2}} \int_0^r \rho(r,t) r^{d-1}\, dr.$$

For the $2 < d < 10$ the results that emerge from a combination of numerical (N) and rigorous (R) analysis are summarized below.

For both bounded and unbounded domains, there are three kinds of eventual behavior that are stable (seen numerically without any tuning of parameters):

(i) Blowup at time T with $h(\eta, t)$ converging to a self-similar profile $H_0(\eta)$ as $t \to T^-$ where the similarity variable $\eta = r/\sqrt{T-t}$. (R,N, see Sec. 4.1 and also Ref. [23]).

(ii) Blowup at time T like a Burgers shock S. This solution is not self-similar – there are two distinct length scales in the solution $R(t) \sim (T-t)^{1/d}$ and $\delta(t) \sim (T-t)^{1-1/d}$. (N, see Sec. 4.2 and also Ref. [14]).

(iii) Steady solutions – In an unbounded domain, the only stable steady solution is $\rho = 0$. A decaying solution on an unbounded domain converges to 0 uniformly on compact sets in both ρ and h. In a bounded domain, if the total mass is sufficiently small, there exists a unique stable steady state $h_0(r)$ (that depends on the total mass). (R, N see Sec. 3).

The blowup modalities in items (i) and (ii) are stable in the sense that the profiles H_0 and S are numerically observed without any tuning of parameters. Of course, blowup solutions are unstable, that is, a small perturbation of the initial condition, unless it is carefully tuned, may lead to a change of the blowup time T, so that the difference between the perturbed and the unperturbed solution can grow without bound.

Besides the stable behaviors, the following asymptotic (that is as $t \to \infty$ for global solutions and $t \to T^-$ for solutions that blow up at T) behaviors of solutions are shown to exist:

(i) A countable family $\{H_n\}, n = 0, 1, \ldots$ of self-similar blowup modalities. H_0 gives a stable blowup profile. In similarity co-ordinates, the profile given by H_n has one unstable mode corresponding to a change in blowup time and at least n additional unstable modes. (R, see Sec. 4.1 and Sec. 5.1).)

(ii) A self-similar blowup modality H_*. It is numerically seen that this blowup modality has one unstable mode corresponding to the blowup time and one additional unstable mode. (N, see Sec. 4.1 and Sec. 5.1.)

(iii) Steady solutions – On an unbounded domain, there exist a one-parameter family of steady solutions, parameterized by ρ_0, the density at the origin, that have $h(r) \to 1$ as $r \to \infty$ that have an infinite number of unstable directions and one neutral direction. These solutions are monotone in ρ but have an infinite number of oscillations in h. (R, N, see Sec. 3). Taking the pointwise limit of $\rho(r)$ or $h(r)$ as $\rho_0 \to \infty$, we obtain a steady solution with a singular density (see. Eq. 18). Taking the limit $\rho_0 \to 0$ yields the steady solution $\rho(r) = 0$.
In a bounded domain, the number of steady solutions is a function of the number $\mu = h(R)$, where h is as defined above and R is the radius of the domain. There exist $N = N(\mu)$ steady solutions $h_0, h_1, \ldots, h_{N-1}$. The solution h_k has k unstable directions. The solution h_0, if it exists, is the stable steady state discussed above. (R, see Sec. 3.)

Numerical results suggest that the codimension one unstable asymptotic behaviors (the solutions with one unstable direction, beside the change in blowup time T) determine the separatrices between the "basins of attractions" of the various stable asymptotic behaviors. We find that each codimension one solutions has connections with a pair of stable solutions and that an initial conditions lying on the boundary between the basins of attractions of different stable behaviors will converge to a codimension one solution asymptotically (see Sec. 6.1). The following connections are observed numerically:

(i) The self-similar blowup modality H_1 has connections to the stable steady state h_0 and to the stable self-similar blow up H_0.

(ii) The self-similar blowup modality H_* has connections with the self-similar blowup H_0 and with the Burger's type shock S.

(iii) The steady solution h_1 has connections with the self-similar blow-up H_0 and the stable steady state h_0.

Figure 4 summarizes these numerical results for the connections between the codimension one behaviors and the stable behaviors. It also presents our conjectures about the existence of connections between the codimension two behaviors the more stable (codimension one and codimension zero) asymtotic behaviors (See Sec. 6.2).

1.2. Outline of the paper

This paper is organized as follows. In Sec. 2 we collect some of the well known properties of solutions of the system in (1). We then describe the existence of an energy functional for the system in (1) on unbounded domains. We also specialize the equations in (1) to the rotationally symmetrical case.

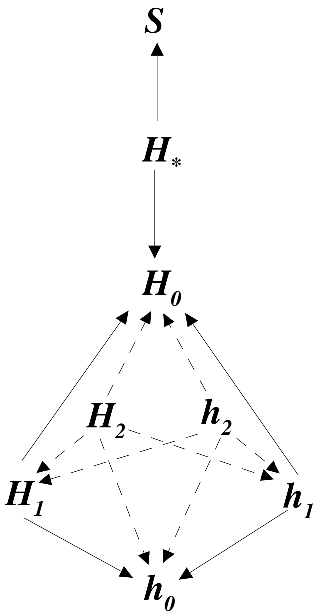

Figure 4. This figure summarizes the connections that we observe numerically (the solid lines) and also some of the connections whose existence we conjecture (the dashed lines) in Sec 6.2.

In Sec. 3 we investigate the radial steady solutions of the system in (1) in both bounded and unbounded domains. In Sec. 4, we first give a proof of blowup of solutions. We then investigate the various kinds of blowup modalities of the system (1). In Sec. 5, we study the stability of the blowup profiles. We discuss the structure of the phase space in Sec. 6.

2. The Energy and comparison principles for solutions

We will first review some of the properties of the solutions of (1). In the solutions to Eq. (1) on $\mathbf{R}^d$, the function c has the representation

$$c(\mathbf{x},t) = \int E(\mathbf{x}-\mathbf{y})\rho(\mathbf{y},t)d\mathbf{y}$$

where E is the fundamental solution of $-\Delta$,

$$E(\mathbf{z}) = -c_2 \log(|\mathbf{z}|)$$

in two dimensions and

$$E(\mathbf{z}) = c_d|\mathbf{z}|^{2-d}$$

in $d \geq 3$ dimensions. We will consider solutions for compactly supported, smooth, non-negative initial data. Positivity and local existence of solutions, for the Cauchy problem with non-negative and rapidly decaying initial data for ρ, follow from minor modifications of standard results for quasilinear parabolic equations [17, 29]. Local existence of solutions for (1) has been shown for a much larger class of initial data (initial data whose norm in a Morrey Space is sufficiently small) in [19] and this result is in a sense optimal.

The equation for ρ in (1) can be written as

$$\partial_t \rho = -\nabla \cdot \Gamma,$$

where the mass-flux Γ is given by

$$\Gamma = -\nabla \rho + \rho \nabla c = -\rho \nabla (\log \rho - c) \tag{2}$$

For the system (1) on a bounded domain Ω, we will impose a no-flux boundary condition and it follows that

$$\int_\Omega \rho(\mathbf{x}, t) d\mathbf{x} = \int_\Omega \rho(\mathbf{x}, 0) d\mathbf{x}.$$

We will denote this conserved quantity by

$$M = M[\rho] = \int_\Omega \rho(\mathbf{x}) d\mathbf{x}.$$

Another property of the equations is scale invariance - On unbounded domains, if $\rho(\mathbf{x}, t)$ is a solution then, for any $L > 0$,

$$\rho_L(\mathbf{x}, t) = L^{-2} \rho(\frac{\mathbf{x}}{L}, \frac{t}{L^2}) \tag{3}$$

is again a solution. To investigate the regularity of the solutions, we will look at the evolution of the $\mathbf{L}^p$ norm of $\rho(r, t)$. From Eq. (1) we obtain

$$\frac{d}{dt} \int \rho^p(\mathbf{x}, t) d\mathbf{x} = -p(p-1) \int |\nabla \rho(\mathbf{x}, t)|^2 \rho(\mathbf{x}, t)^{p-2} d\mathbf{x} + (p-1) \int \rho(\mathbf{x}, t)^{p+1} \tag{4}$$

At $p = \frac{d}{2}$ the growth term in the RHS can be bound in terms of the dissipation term by

$$\int \rho^{\frac{d+2}{2}}(\mathbf{x}, t) d\mathbf{x} \leq C \left(\int |\nabla \rho(\mathbf{x}, t)|^2 \rho(\mathbf{x}, t)^{\frac{d-4}{2}} d\mathbf{x} \right) \left(\int \rho^{\frac{d}{2}}(\mathbf{x}, t) d\mathbf{x} \right)^{2/d}.$$

This inequality follows from the Sobolev inequality (*cf.* Evans and Gariepy [32]) by straightforward interpolation (or Hölder inequality). This is a modification of a similar estimate for the Keller-Segel system obtained in [17]. A consequence of this is the fact that if the initial $\mathbf{L}^{\frac{d}{2}}$ norm of ρ is small then it is non-increasing in time; higher norms can be shown to decay also. This proves the regularity of solutions for initial data whose $\mathbf{L}^{\frac{d}{2}}$ norm is sufficiently small. It is also known that if any of the $\mathbf{L}^p$ norms of ρ diverge, then all the norms for $p \geq d/2$ diverge simultaneously [4].

2.1. The Energy in unbounded domains

Consider the quantity

$$\mathcal{E}(\rho) = \int \left((\rho(\mathbf{x}) \log(\rho(\mathbf{x})) - \rho(\mathbf{x})) - \frac{1}{2}\rho(\mathbf{x})c(\mathbf{x}) \right) d\mathbf{x}. \tag{5}$$

Note that in more than two dimensions the integral of ρc is positive and always

$$\int \rho c d\mathbf{x} = \int \int E(\mathbf{x} - \mathbf{y})\rho(\mathbf{x})\rho(\mathbf{y}) d\mathbf{x} d\mathbf{y}$$

The quantity $\mathcal{E}(\rho(\cdot, t))$ decays on solutions

$$\frac{d}{dt} \int \left(\rho(\log \rho - 1) - \frac{1}{2}\rho c \right) d\mathbf{x} = -\int \rho |\nabla(\log \rho - c)|^2 d\mathbf{x} = -\int \frac{\Gamma^2}{\rho} d\mathbf{x}.$$

Therefore, the energy dissipation vanishes only if the mass flux $\Gamma = 0$, so that ρ is a steady (time-independent) solution. Similar Lyapunov functionals have been used in the analysis of the system in (1) as well as the Keller-Segel system, on bounded as well as unbounded domains, in Refs. [24], [25] and [26]. The existence of a Lyapunov functional implies that (1) does not have any periodic solutions with $\mathcal{E}$ finite. Therefore, every solution of (1) with a finite energy that is global in time has to converge to a steady (time-independent) solution. Another possibility is for the solution to have a finite time singularity so that the solution cannot be extended beyond the blowup time.

Note that, the functional derivative of $\mathcal{E}$ is

$$\frac{\delta \mathcal{E}}{\delta \rho} = \log \rho - c$$

so the equation takes the form

$$\partial_t \rho = \nabla \cdot \left(\rho \nabla \frac{\delta \mathcal{E}}{\delta \rho} \right) \tag{6}$$

The energy can be used to deduce information about steady states. If the energy and energy dissipation are well defined then the latter must vanish for time independent solutions. In the whole space the implications are the following: if ρ is the density of a smooth steady state and if it is strictly positive in an unbounded open connected set then it follows that $\log \rho - c$ is a constant in the same set. This implies that $\rho = k \exp(c)$ and because c vanishes at infinity it follows that ρ does not. This is impossible if the energy is finite, so the assumptions are inconsistent: there are no steady states with a finite energy on an unbounded domain.

2.2. Radial Equations

We will henceforth restrict ourselves to solutions with spherical symmetry and treat the space dimension d as a parameter in the equation. Let $m(r, t)$ be given by

$$m(r, t) = \int_0^r \rho(r, t) r^{d-1} dr, \tag{7}$$

so that $m(r)$ is the mass inside a sphere of radius r divided by $C_d = d\pi^{d/2}/\Gamma((d+2)/2)$ (the "surface area" of the unit sphere in d dimensions). From the system in Eq. (1), we can deduce that $m(r,t)$ satisfies

$$\partial_t m = \partial_r^2 m - \frac{d-1}{r}\partial_r m + \rho m. \tag{8}$$

Under a scale transformation $r \to r/L, t \to t/L^2$, the transformation of the quantity m is given by

$$m_L(r,t) = L^{d-2} m\left(\frac{r}{L}, \frac{t}{L^2}\right)$$

In the variable ρ, we have the integro-differential equation

$$\partial_t \rho = \partial_r^2 \rho + \frac{d-1}{r}\partial_r \rho + \frac{1}{r^{d-1}}\partial_r(m\rho). \tag{9}$$

The boundary conditions are ρ decaying at infinity for unbounded domains and zero mass flux at the boundaries for bounded domains.

All the numerical results we present in this paper are for solutions on bounded domains. We use (9) along with the definition of m in (7) and the no-flux boundary conditions for our numerical simulations. All the simulations were done using a mass conserving, second-order in time step, implicit scheme along with adaptive mesh refinement. Some of the numerical results reported in this paper were obtained with numerical routines that were developed using BuGS [30], a general purpose toolkit for solving parabolic PDEs.

We define the quantities $b(r)$ and $h(r)$ by

$$b(r) = \frac{dm(r)}{r^d}, \tag{10}$$

and

$$h(r) = \frac{m(r)}{2r^{d-2}}. \tag{11}$$

Under a scale transformation, b transforms like ρ *i.e.*,

$$b_L(r,t) = \frac{1}{L^2} b\left(\frac{r}{L}, \frac{t}{L^2}\right),$$

and h transforms as

$$h_L(r,t) = h\left(\frac{r}{L}, \frac{t}{L^2}\right).$$

so that h does not pick up any powers of L under a scale transformation. The variables b and h turn out to be the most convenient variables to analyze this system. $b(r,t)$ satisfies the equation

$$\begin{aligned}\partial_t b(r,t) &= \Delta_{d+2} b(r,t) + \rho b(r,t) \\ &= \partial_r^2 b(r,t) + \left(\frac{d+1}{r} + \frac{rb(r,t)}{d}\right)\partial_r b(r,t) + b^2(r,t),\end{aligned} \tag{12}$$

where

$$\Delta_{d+2} = \partial_r^2 + \frac{d+1}{r}\partial_r$$

is the $d+2$ dimensional radial Laplacian. $h(r,t)$ satisfies the equation

$$\partial_t h(r,t) = \partial_r^2 h(r,t) + \left(\frac{d-3+2h(r,t)}{r}\right)\partial_r h(r,t) + \frac{2(d-2)h(r,t)}{r^2}(h(r,t)-1) \quad (13)$$

2.3. Comparison principles for radial solutions

As a consequence of the maximum principle for parabolic equations [31], we obtain the following comparison principles for the radial solutions of (1):

(i) The number of oscillations of the density $\rho(r,t)$ (the number of changes of sign in $\rho_r(r,t)$) is non-increasing in time.

(ii) The number of changes of sign of $h_1(r,t) - h_2(r,t)$ is non-increasing for any pair of non-negative solutions $h_1(r,t)$ and $h_2(r,t)$.

These results are obtained by adapting the proofs for similar results in Ref. [29]. A consequence of (ii) is the following:

Let $m_1(r,t)$ and $m_2(r,t)$ be solutions to Eqs. (7) and (8) on a domain Ω. If $m(r,t_0) \le m_S(r,t_0)$ holds at some time t_0 for all $r \in \Omega$ then $m(r,t) \le m_S(r,t)$ for all $t \ge t_0$.

3. Time independent solutions

We will now investigate the steady (time-independent) solutions of Eq. (8). The steady solutions $\bar{m}(r)$ are given by

$$r^{d-1}\left(\frac{\bar{m}'}{r^{d-1}}\right)' + \bar{\rho}\bar{m} = 0 \quad (14)$$

Using Eq. (7), the above equation can be written as the following system of coupled ODEs

$$\bar{\rho}' = -\frac{\bar{\rho}\bar{m}}{r^{d-1}}, \qquad \bar{m}' = \bar{\rho}r^{d-1}. \quad (15)$$

The steady states are solutions to the ODEs with the initial conditions

$$\bar{\rho}(0) = \rho_0, \lim_{r\to 0}\frac{d\bar{m}(r)}{r^d} = \rho_0 \quad (16)$$

The solutions to these ODEs give us a one-parameter family of steady solutions parameterized by the density at the origin ρ_0. These solutions are related to each other by the scale transformation

$$r \to r/L, \rho_L(r) = L^{-2}\rho(r/L)$$

Consequently, we can obtain all the steady solutions by integrating the system of equations in (15) with $\rho_0 = 1$ and rescaling appropriately.

3.1. Steady solutions in $d > 2$

Let $m_S(r)$ be the solution of Eq. (14) for a particular value of ρ_0. Then we have the following result:

Theorem 1. *For $d > 2$, we have*

$$h_S(r) = \frac{m_S(r)}{2r^{d-2}} \to 1 \text{ as } r \to \infty.$$

Further, for $2 < d < 10$, the solution $h_S(r)$ has a countable number of oscillations about the asymptotic value of $h = 1$ and for $d > 10$, the solution is monotonic on $(0, \infty)$.

This result is obtained by doing a phase-plane analysis of the autonomous system that is obtained for h in the variable $z = \log(r)$ (See [18]).

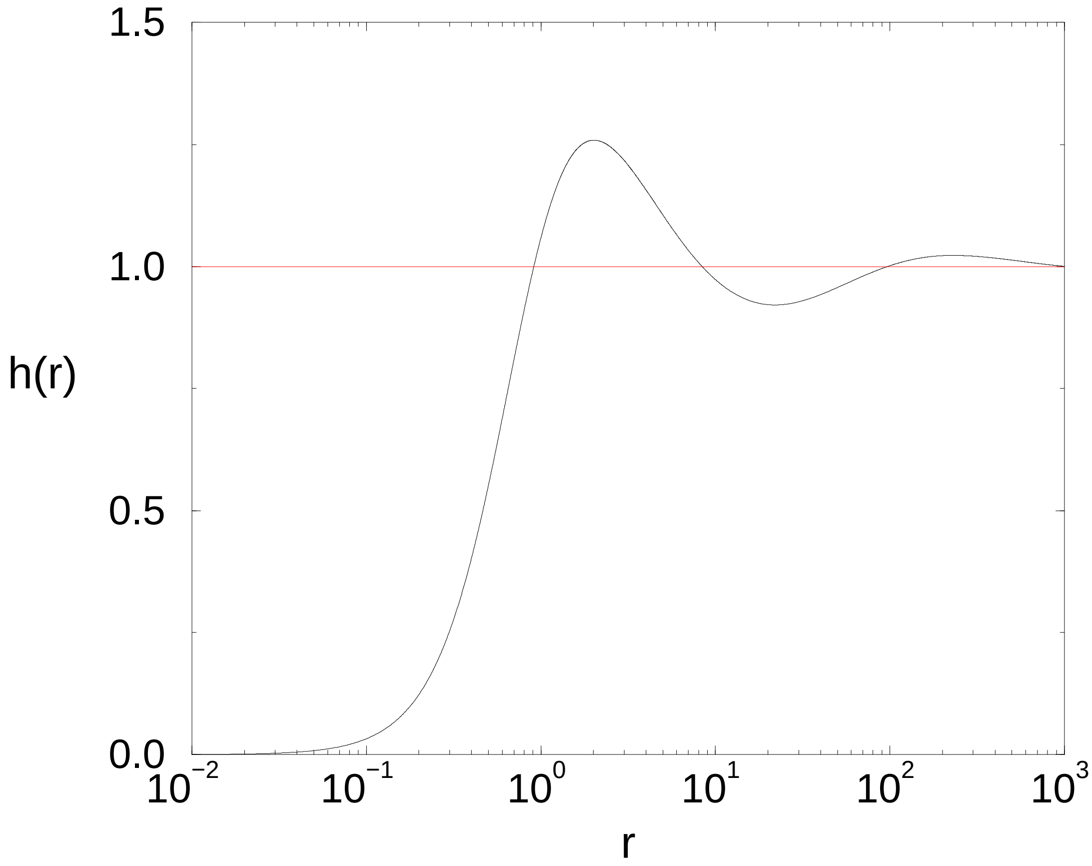

Figure 5. h_S as a function of r for $d = 3$. $\rho_0 = 20$

Since all steady solutions are related by scale transformations, the one parameter family of steady solutions is given by $h_L(r) = h_S(r/L)$, where h_S is the particular steady solution from above and L is a continuous parameter. For all these steady solutions, $m_L(r)$ asymptotically given by

$$\bar{m}_L(r) = 2r^{d-2}, \tag{17}$$

independent of the initial density ρ_0. Therefore, there are no finite mass steady state solutions for $d > 2$ on an unbounded domain. There are however finite mass steady solutions on bounded domains. Fig. 5 shows a plot of h_S as a function of r for $d = 3$. The density at the origin is $\rho_0 = 20$.

Taking the limit $L \to 0$, $h_S(r/L)$ converges pointwise to the solution $h(r) = 1$. This is a steady solution that corresponds to a singular density of the form

$$\rho(r) = 2(d-2)r^{-2} \tag{18}$$

and is called the Chandrasekhar solution [19]. Taking the limit $L \to \infty$, we $h_S(r/L)$ converges to $h(r) = 0$ uniformly on compact sets. These limiting solutions are important in the study of the behavior of solutions of (1) on unbounded domains.

We will now investigate the conditions under which there exist steady solutions in a bounded domain B_R (the ball with radius R) in d dimensions with a given total mass M. We define the quantity

$$\mu = h(R) = \frac{M}{2C_d R^{d-2}},$$

where C_d as defined above is the "area" of a unit sphere in d dimensions. Since all the steady solutions can be obtained by appropriate scale transformations of a particular steady solution (say the solution $h_S(r)$), it follows that there exists a steady solution in B_R with a total mass M if and only if we can find a r_μ such that

$$h_S(r_\mu) = \mu \tag{19}$$

For $2 < d < 10$, let μ_i represent the ith extremum of the curve $h_S(r)$ with $r \in (0, \infty)$, *i.e.* not counting the point $(0, 0)$ and let $\mu_0 = 0$. From the phase plane analysis, it is easily seen that

$$\mu_1 > \mu_3 > \mu_5 > \ldots > 1,$$

and

$$0 = \mu_0 < \mu_2 < \mu_4 < \mu_6 < \ldots < 1.$$

(See Fig. 5 for an illustration of these inequalities for $d = 3$). Consequently, there are no solutions to Eq. (19) if $\mu > \mu_1$. There is one solution for $\mu_0 = 0 < \mu < \mu_2$, two solutions for $\mu_3 < \mu < \mu_1$ and so on.

Let r_i denote the $i + 1$th solution to Eq. (19), *i.e*, r_i is in between $h_S^{-1}(\mu_i)$ and $h_S^{-1}(\mu_{i+1})$. The scale factor L for obtaining the solution in the bounded domain B_R is given by

$$L_i = R/r_i.$$

Therefore, for every solution r_i of Eq. (19), we can find a steady solution in B_R given by

$$h_i(r) = h_S\left(\frac{r_i}{R} r\right)$$

Note that $h_i(r)$ has i extrema in $(0, R)$.

Also note that, if $\mu = 1$, $\lim_{i\to\infty} h_i(r)$ exists pointwise, and the limiting function corresponds to the Chandrasekhar solution (18).

If $M > M_c$ with

$$M_c = 2\mu_1 C_d R^{d-2}, \tag{20}$$

Eq. (19) has no solutions. Consequently, there exists a critical mass M_c such that there exist no spherically symmetric steady solutions in a bounded domain B_R with a mass larger than M_c [18]. From the above discussion, it is also clear that if μ is such that a steady solution exists, then the steady solution is not necessarily unique [18].

For $d > 10$, the $h_S(r)$ increases monotonically from 0 to 1. Therefore, there exist no steady solutions with mass larger than $M_c = 2C_d R^{d-2}$ for a space dimension d. In this case however, if a steady solution exists with a given mass, it is unique [18].

3.2. Stability of steady solutions in a bounded domain

As we saw above, we can have more than one steady solution with a given total mass and a given bounded domain B_R in dimensions $2 < d < 10$. We will now prove the following result concerning the stability of the various steady solutions.

Theorem 2. *: Let $\mu = M/(2R^{d-2})$ be such that there exist p steady solutions $h_0(r), h_1(r), \ldots, h_{p-1}(r)$ with the given total mass on the bounded domain B_R. Then, the solution $h_i(r)$ that has i extrema for $r \in (0, R)$ with $i \geq 1$ is unstable and the corresponding unstable manifold has a dimension i.*

Proof. Linearizing Eq. (13) about $h = h_i$, we obtain

$$\begin{aligned}\partial_t\phi(r,t) = \partial_r^2\phi(r,t) + \left(\frac{d-3+2h_i(r,t)}{r}\right)\partial_r\phi(r,t)\\ + \frac{2r\partial_r h_i(r) + 2(d-2)(2h_i(r)-1)}{r^2}\phi(r,t)\end{aligned} \tag{21}$$

We will consider the eigenvalue problem for the above equation. let ϕ_λ be a solution of

$$\begin{aligned}&\partial_r^2\phi_\lambda(r) + \left(\frac{d-3+2h_i(r,t)}{r}\right)\partial_r\phi_\lambda(r)\\ &+ \left[\frac{2r\partial_r h_i(r) + 2(d-2)(2h_i(r)-1)}{r^2} + \lambda\right]\phi_\lambda(r) = 0\end{aligned} \tag{22}$$

with the initial conditions

$$\phi_\lambda(r) \to r^2 \text{ as } r \to 0.$$

We are interested in finding λ_n so that the solution $\phi_{\lambda_n}(r)$ satisfies $\phi_{\lambda_n}(R) = 0$. If we define $\psi_\lambda(r) = \phi_\lambda(r)v(r)$, where $v(r)$ is given by

$$v(r) = \exp\left[\frac{1}{2}\int_1^r \frac{d-3+2h_i(r_1)}{r_1}\,dr_1\right],$$

$\psi_\lambda(r)$ satisfies the equation

$$\partial_r^2\psi_\lambda(r) + (q(r)+\lambda)\psi_\lambda(r) = 0$$

with

$$q(r) = \left[\frac{4r\partial_r h_i(r) + 8(d-2)(2h_i(r)-1) + 1 - (d-2+2h_i(r))^2}{r^2}\right].$$

Off the origin, $v(r) > 0$. Therefore, the zeroes of ψ_λ and ϕ_λ coincide off the origin. Also, if $\lambda_m > \lambda_n$, by the Sturm comparison theorem, ψ_{λ_m} vanishes between every two zeroes of ψ_{λ_n} and therefore, it is also true that ϕ_{λ_m} vanishes between every two zeroes of ϕ_{λ_n}. It is easily seen that the locations of the zeroes of ϕ_λ are continuous functions of λ.

Setting $h = h_i(r/L)$ in Eq. (13) with L arbitrary, yields an identity since the steady solutions are scale invariant. Differentiating this identity *w.r.t.* L and setting $L = 1$, it is easily seen that $f_0(r) = rh_i'(r)$ satisfies Eq. (22) with $\lambda = 0$ so that $\phi_0(r) = f_0(r)$. The function $h_i(r)$ has i extrema in $(0, R)$. Therefore, the function $\phi_0(r)$ has i zeroes in the open set $(0, R)$. By the Sturm comparison theorem and the continuity of the location of the zeroes as a function of λ, there exists a $\lambda^*_{-1} < 0$ such that $\phi_{\lambda^*_{-1}}(R) = 0$ and there are exactly $i-1$ zeroes for $\phi_{\lambda^*_{-1}}(r)$ in $(0, R)$ and a $\lambda^*_0 \geq 0$ such that $\phi_{\lambda^*_0}(R) = 0$ and there are exactly i zeroes for $\phi_{\lambda^*_0}(r)$ in $(0, R)$.

Now, by standard results from Sturm-Liouville theory, it follows that there exist $\lambda^*_{-i} < \ldots < \lambda^*_{-2} < \lambda^*_{-1} < 0$ such that $\phi_{\lambda^*_{-k}}(R) = 0$ and $\phi_{\lambda^*_{-k}}(r)$ has exactly $i-k$ zeroes in $(0, R)$.

All the eigenfunctions with eigenvalues less than zero are unstable.This proves our claim that the steady solution $h_i(r)$ is unstable for $i \geq 1$ and the unstable manifold has dimension i. □

4. Blowup modalities

In the previous section, we analyzed the time-independent (steady) solutions of the system (1). In this section, we will investigate time-dependent solutions with finite time singularities. We begin by showing that there exist spherically symmetric solutions that blow up in a finite time for $d \geq 2$.

Theorem 3. *For $d \geq 2$, there exist solutions of the radial equations (8) such that the density blows up at a finite time,* i.e., *we can find sequences $r_n \to r^*$ and $t_n \to T^* < \infty$ such that* $\limsup_{n\to\infty} \rho(r_n, t_n) = \infty$.

Proof. For radial solutions, Eq. (12) gives

$$\partial_t b(r,t) = \Delta_{d+2} b(r,t) + \rho b(r,t), \tag{23}$$

where

$$\Delta_{d+2} = \partial_r^2 + \frac{d+1}{r}\partial_r \tag{24}$$

is the $d+2$ dimensional radial Laplacian. Now we take a function γ that depends on a free parameter T

$$\gamma(r,t) = c_{d+2}(T-t)^{-\frac{d+2}{2}} \exp\left[-\frac{r^2}{4(T-t)}\right]. \tag{25}$$

This function solves the backward $d+2$ dimensional heat equation with final condition $\gamma(\cdot, T) = \delta$. The constant c_{d+2} is adjusted so that

$$\int_0^\infty \gamma(r,t) r^{d+1} dr = 1.$$

We note for later use that

$$\partial_r \gamma = -\frac{r}{2(T-t)}\gamma.$$

The constant T will be chosen later. Now we multiply the equation (23) by γ, integrate $r^{d+1}dr$ and use the properties of γ. After checking that there are no boundary contributions we obtain:

$$\frac{d}{dt}\int_0^\infty b(r,t)\gamma(r,t)r^{d+1}dr = \int_0^\infty \rho(r,t)b(r,t)\gamma(r,t)r^{d+1}dr.$$

We recall that

$$r^{d-1}\rho = \partial_r m$$

and that

$$r^d b(r,t)/d = m.$$

We deduce

$$\frac{d}{dt}\int_0^\infty b(r,t)\gamma(r,t)r^{d+1}dr = \frac{1}{2d}\int_0^\infty \left[\frac{r^2}{2(T-t)} + (d-2)\right] b^2(r,t)\gamma(r,t)r^{d+1}dr. \tag{26}$$

Now, if $d > 2$ we discard the first term in the square brackets and use the fact that

$$\left(\int b(r)\gamma(r)r^{d+1}dr\right)^2 \le \int b(r)^2\gamma(r)r^{d+1}dr$$

that follows from the positivity and normalization of γ via the Schwartz inequality. Therefore the quantity

$$y(t) = \int_0^\infty b(r,t)\gamma(r,t)r^{d+1}dr$$

obeys the inequality

$$\frac{d}{dt}y \ge \frac{d-2}{2d}y^2.$$

Consequently this quantity diverges no later than $t = T_\infty$ where

$$T_\infty = \frac{2d}{d-2}\frac{1}{y(0)}.$$

Now we will choose T and the initial data so that

$$T_\infty < T$$

and conclude that we have blowup in $d > 2$. Recalling that

$$y(0) = dc_{d+2} \int_0^\infty T^{-\frac{d+2}{2}} \exp\left(-\frac{r^2}{4T}\right) m_0(r) r dr,$$

using the definition of m and changing the order of integration we obtain that

$$y(0) = 2dc_{d+2} T^{-\frac{d}{2}} \int_0^\infty \rho_0(r) \exp\left(-\frac{r^2}{4T}\right) r^{d-1} dr.$$

By choosing first $T > 0$ and then ρ_0 appropriately, for instance

$$\rho_0(r) = N$$

for $r \leq T^{-\frac{1}{2}}$ and $\rho_0 = 0$ for the rest we deduce that $T_\infty < T$ follows from

$$N dc_{d+2} \int_0^1 \exp\left(-\frac{x^2}{4}\right) x^{d-1} dx > \frac{1}{T(d-2)},$$

i.e., if NT is sufficiently large. If $d = 2$ the analysis is based on the slightly different inequality

$$\left(\int_0^\infty b(r,t)\gamma(r,t) r^3 dr\right)^2 \leq C \int_0^\infty b(r,t)^2 \gamma(r,t) \frac{r^2}{2(T-t)} r^3 dr$$

with $C = 4c_4$ but otherwise it is completely similar.

□

Note that the *blowup quantity* $y(t)$ is actually a priori bounded in terms of the conserved mass. However, its time derivative is not bounded, and the argument in Theorem 3 implies that the quantity $y(t)$ has to develop a discontinuity (shock) before the time T_∞.

Various authors have proved the existence of solutions that blowup for the system in (1) as well as the Keller-Segel equations and other generalizations of these equations, both for radial and non-radial solutions, using a variety of techniques. Some of these proofs can be found in references [17], [18], [20] and [33].

4.1. Self-similar blowup

The scale invariance (See Eq. (3))

$$r \to r/L, \rho_L(r,t) = L^{-2} \rho(r/L, t/L^2)$$

motivates us to look for solutions with the parabolic scaling

$$L \sim \sqrt{T-t}. \tag{27}$$

for solutions that blow up at $t = T$. We look for solutions of the form

$$\rho(r,t) \sim \frac{1}{T-t} \Pi\left(\frac{r}{\sqrt{T-t}}\right) \tag{28}$$

subject to the boundary conditions

$$\Pi(\eta) \to 0 \text{ as } \eta \to \infty \quad \text{and} \quad \Pi(0) < \infty. \tag{29}$$

To look for solutions that blow up, we rewrite the equations in terms of the scaled radial coordinate $\eta = r/\sqrt{T-t}$ and the slow time $\tau = -\log(T-t)$, and we obtain

$$\partial_\tau \Pi = \partial_\eta^2 \Pi + \frac{d-1}{\eta}\partial_\eta \Pi + \frac{1}{\eta^{d-1}}\partial_\eta(\tilde{m}(\eta)\Pi) - \Pi - \frac{1}{2}\eta\partial_\eta \Pi, \tag{30}$$

where $\tilde{m}(\eta) = \int_0^\eta \xi^{d-1}\Pi(\xi)d\xi$.

It is again convenient to solve for the function $h(r,t)$ instead of $\rho(r,t)$. Taking note of the rescaling properties of $h(r,t)$, we write $h(r,t) = H(\eta,\tau)$. We imagine that $H(\eta,\tau) = H_S(\eta) + H_C(\eta,\tau)$, where $H_S(\eta)$ is a self-similar solution that describes the blowup and $H_C(\eta,\tau)$ describes the approach to the self-similar solution, so that $H_C(\eta_0,\tau) \to 0$ as $\tau \to \infty$ for any fixed $\eta_0 < \infty$. In the rescaled coordinates, we can rewrite Eq. (13) as

$$\begin{aligned} \partial_\tau H(\eta,\tau) = \partial_\eta^2 H(\eta,\tau) + \left(\frac{d-3+2H(\eta,\tau)}{\eta}\right)\partial_\eta H(\eta,\tau) \\ + \frac{2(d-2)H(\eta,\tau)}{\eta^2}(H(\eta,\tau)-1) - \frac{\eta}{2}\partial_\eta H(\eta,\tau). \end{aligned} \tag{31}$$

The τ independent solutions of this equation that satisfy the boundary conditions

$$\eta\partial_\eta H_S(\eta) \to 0 \text{ as } \eta \to \infty \quad \text{and} \quad \lim_{\eta\to 0}\frac{H_S(\eta)}{\eta^2} < \infty,$$

give exactly self-similar solutions that blow up at a finite time T. If we set $\partial_\tau H_S(\eta) = 0$ in (31), we obtain

$$\partial_\eta^2 H_S + \left[\frac{d-3+2H_S}{\eta} - \frac{\eta}{2}\right]\partial_\eta H_S + \frac{2(d-2)(H_S-1)H_S}{\eta^2} = 0. \tag{32}$$

Besides satisfying the boundary conditions at infinity and at $\eta = 0$, in order to describe the blowup of a solution whose initial condition is a non-negative density, we need that the solution H_S should have a non-negative density and a non-negative mass for all $\eta \geq 0$, *i.e.*, $H_S \geq 0$ and $\partial_\eta(\eta^{d-2}H_S) \geq 0$.

Fig. 6 shows numerically obtained solutions to Eq. (32) that satisfy the boundary conditions and also have a non-negative mass and density.

We have the following theorem about the solutions to Eq. (32).

Theorem 4. *For $2 < d < 10$, there exist a countable number of solutions to the equation*

$$\partial_\eta^2 H_S + \frac{d-3+2H_S}{\eta}\partial_\eta H_S + \frac{2(d-2)H_S}{\eta^2}(H_S-1) - \frac{\eta}{2}\partial_\eta H_S = 0,$$

satisfying the boundary conditions $H_S(\eta)/\eta^2$ is bounded as $\eta \to 0$ and $\eta\partial_\eta H_S \to 0$ as $\eta \to \infty$ and the requirements $H_S(\eta) \geq 0$, $\partial_\eta(\eta^{d-2}H_S(\eta)) \geq 0$ for all η.

These solutions are characterized by the number of intersections with the line $H = 1$. More precisely, given a non-negative integer N, there exists at least one $U \in [-1,1]$ and a solution H_N such that the solution $H_N(\eta)$ intersects the line $H = 1$ precisely $N+1$ times and $\lim_{\eta\to\infty} H(\eta) = 1 + U$.

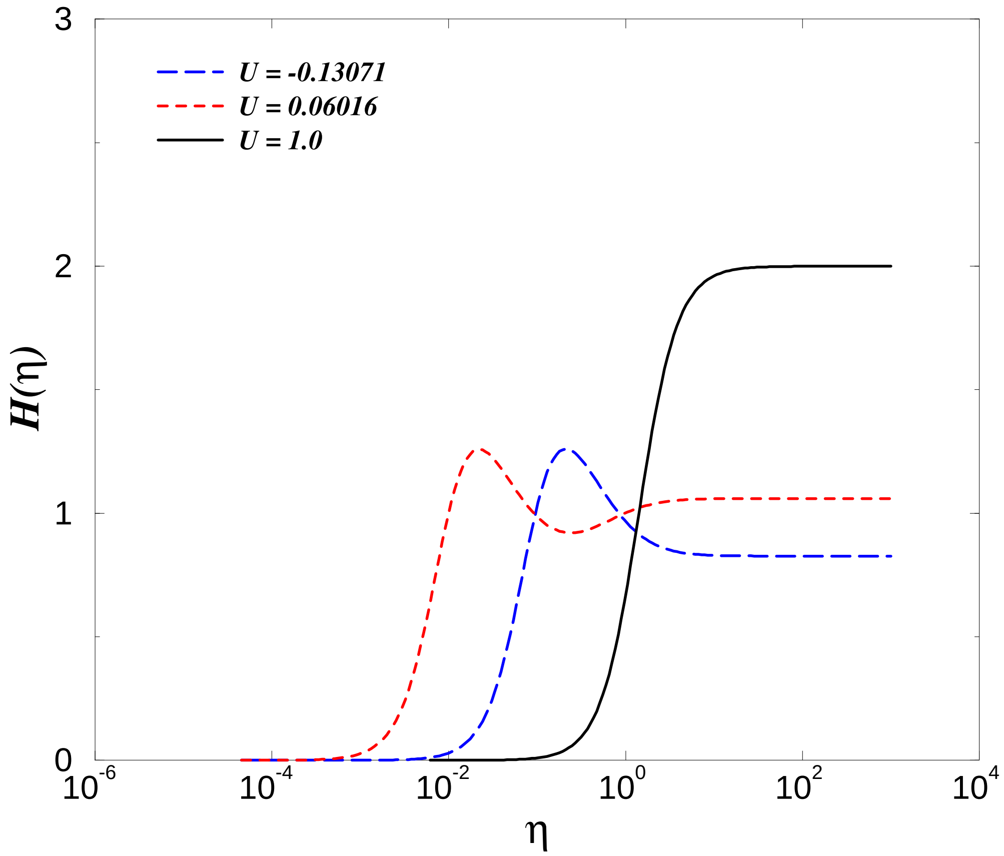

Figure 6. Similarity solutions for the blowup profiles for $d = 3$. The similarity solutions satisfy $\lim_{\eta\to\infty} H(\eta) = 1 + U$. The figure shows solutions with $N = 1, 2$ and 3 intersections with the line $H = 1$.

This theorem can be proved using a shooting argument. The proof is obtained using the following results:

(i) For any $U \in [-1, 1]$ with $U \neq 0$, there exists an $\eta_1(U) \geq 0$ such that Eq. (32) has a nonnegative solution on (η_1, ∞) with $\lim_{\eta\to\infty} H = 1 + U$. This solution has $\Pi(\eta) \geq 0$ for $\eta \in (\eta_1, \infty)$ (non-negative density) and is maximal in the sense that $H(\eta_1) = 0$ and if $\eta_1 > 0$, any extension of the solution for $\eta < \eta_1$ will make H negative.

(ii) For any $U \in [-1, 1]$ with $U \neq 0$, the solution constructed above has a finite number of intersections, $N(U)$, with the line $H = 1$ on the interval (η_1, ∞).

(iii) If $\eta_1(U_a) > 0$, there is a connected neighborhood of U_a where $N(U)$ is a constant. On this neighborhood, η_1 and the locations of the intersections depend continuously on U.

(iv) If U_a is such that no open neighborhood of U_a has a constant $N(U)$, it follows that $\eta_1(U_a) = 0$, $H(0) = 0$, $\Pi(0) < \infty$, we can choose an open neighborhood of U_a sufficiently small so that $N(U)$ attains only two distinct values on this neighborhood, and these values differ by 2.

(v) We can write down explicit solution with $N(U_a) = 1$ ($U_a = 1$) and $N(U_b) = 0$ ($U_b = -1$).

(vi) Given any natural number M, we can find a U sufficiently close to 1 such that $N(U) > M$. Also, $N(U)$ is odd for $U > 0$ and even for $U < 1$.

These results are proved in Ref. [34]. From these results, it is easily seen that, given any natural number N, there exists at least one solution of (32) that satisfies the boundary conditions, and has N intersections with the line $H = 1$. In the proof, we also obtain that the solution with N intersections has precisely $N - 1$ extrema for $\eta \in (0, \infty)$. As in the statement of the theorem, we will denote this solution by H_{N-1}. These solutions give self-similar blowup modalities for (1). They have also been described in Ref. [23].

Remark 1 The theorem as stated guarantees the existence of a solution H_N having $N+1$ intersections with the line $H = 1$ for any given integer $N \geq 0$, but it does not make any claims on the uniqueness of such solutions. Numerical evidence suggests that the solution H_N with $U = \lim_{\eta\to\infty} H_N(\eta) - 1 \in [-1, 1]$ is unique. If, however, we relax the restriction that $U \in [-1, 1]$, it turns out that the solutions are not necessarily unique. We will return to this point subsequently.

Remark 2 It is easily seen that, for $d > 2$, all the solutions to Eq. (32) satisfying the boundary conditions describe blowup where the density diverges at the origin but no mass is concentrated at the origin, *i.e.*,

$$\lim_{\epsilon\to 0}\left(\lim_{t\to T} m(\epsilon, t)\right) = 0.$$

For all $d > 2$, we can check that

$$H_0(\eta) = \frac{2\eta^2}{2(d-2) + \eta^2} \tag{33}$$

is a solution of Eq. (32) satisfying the boundary conditions and the non-negativity requirements. This solution has $U = 1$ and $N = 1$ (one intersection with the line $H = 1$.)

We will show below that all the stable self-similar blowup profiles should have no extrema for $\eta \in (0, \infty)$ so that they can have no more than one intersection with the line $H = 1$. Therefore, all the other solutions to Eq. (32) for $2 < d < 10$, that are described in Theorem 4, give blowup profiles that are unstable.

Fig. 7 shows numerically obtained solutions to Eq. (1) with spherical symmetry for $d = 3$. The figure shows the density scaled by the inverse of the time to blowup as a function of the radial coordinate rescaled by the square root of the time to blowup.

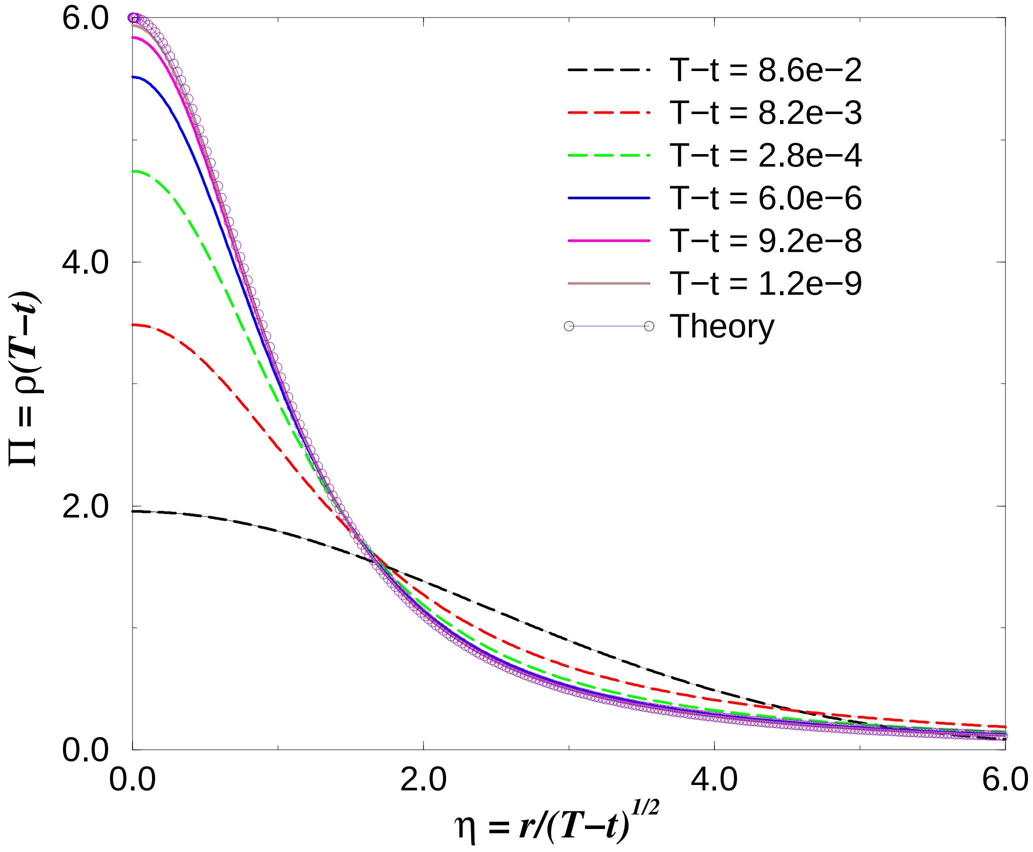

Figure 7. Blowup profile for $d = 3$. The solution converges in similarity variables to the theoretical profile given by Π_1. The blowup time T is estimated using the density at the origin.

This is precisely the scaling in Eq. (28). The theoretical curve is given by the density corresponding to the solution $H_0(\eta)$ in Eq. (33), *i.e.*,

$$\Pi_0(\eta) = \frac{4(d-2)(2d+\eta^2)}{[2(d-2)+\eta^2]^2}. \tag{34}$$

We find that this blowup profile is stable in the sense that there is an open set of initial conditions all of which blow up converging to this profile.

As we remarked earlier, the solutions with $N = 1$ are not unique if we relax the restriction that $U \in [-1, 1]$. Figure 8 shows $H_*(\eta)$, a solution of Eq. (32) for $d = 3$ satisfying the boundary conditions with $U = 16.378\ldots$. Also shown is the solution $H_0(\eta)$ given by (33). Both these solutions have $N = 1$ and have no extrema for $\eta \in (0, \infty)$ in contrast to the solutions $H_N(\eta)$ with $N \geq 1$ whose existence is guaranteed by Theorem 4.

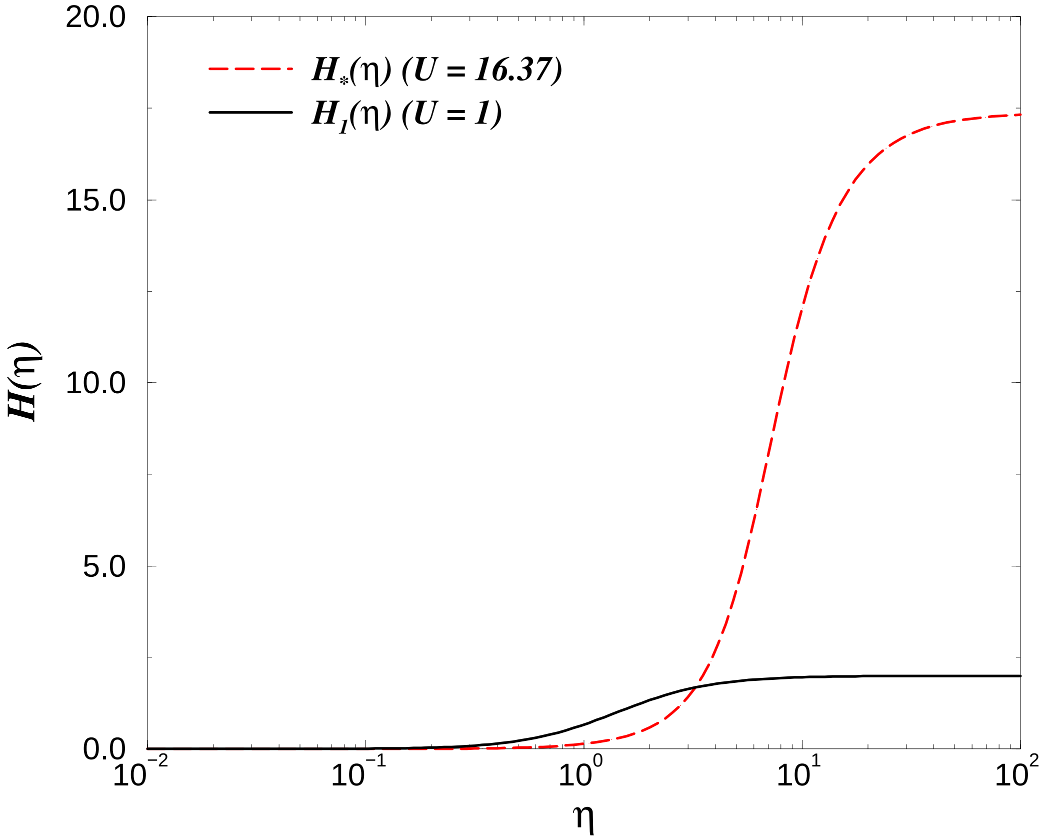

Figure 8. Similarity solutions for $d = 3$. This figure shows the solutions $H_0(\eta)$ and $H_*(\eta)$ that have $N = 1$.

4.2. Non Self-similar blowup

In this section, we present numerical results about certain solutions $\rho(r, t)$ that blow up in a non self-similar fashion. By non self-similar, we mean that the asymptotics of such solutions do not develop on scales corresponding to the similarity variables $\eta = r/\sqrt{T - t}$ and $\Pi = (T - t)\rho$. They correspond to an imploding smoothed out shock wave that collapses into a Dirac mass at the origin when the singularity is formed. Hence, unlike the self-similar solutions described above, a finite portion of the initial mass is driven to the origin at the blowup time. For $d = 3$, those solutions have been analyzed in [14] by means of matched asymptotics.

As mentioned in the previous section, the density profile Π_1 given by the explicit similarity solution in (34) has been obtained numerically for several initial data with the density concentrated in balls around the origin or in shells close enough to the origin. On the other hand, starting with an initial condition whose mass is concentrated in a shell away from the origin, the numerical integration of Eq. (9) does not lead to this self-similar blowup, but to the formation of a peak moving towards the origin, with a height blowing up to infinity and a width shrinking to zero at a finite time T.

This behavior is also stable in the sense that it has been observed for various such initial data, so that it is expected for an open set of initial conditions. Figure 3 shows a typical profile just prior blowup. Furthermore, the dynamics of the height $Q(t)$ of the peak, its width $\delta(t)$ and its location $R(t)$ depend upon the dimension d and satisfy for several values of $d > 2$, as $t \to T$,

$$Q(t) = c_1(T-t)^{-2\frac{d-1}{d}}, \quad \delta(t) = c_2(T-t)^{\frac{d-1}{d}}, \quad R(t) = c_3(T-t)^{1/d}. \quad (35)$$

See Figs. 9, 10 and 11.

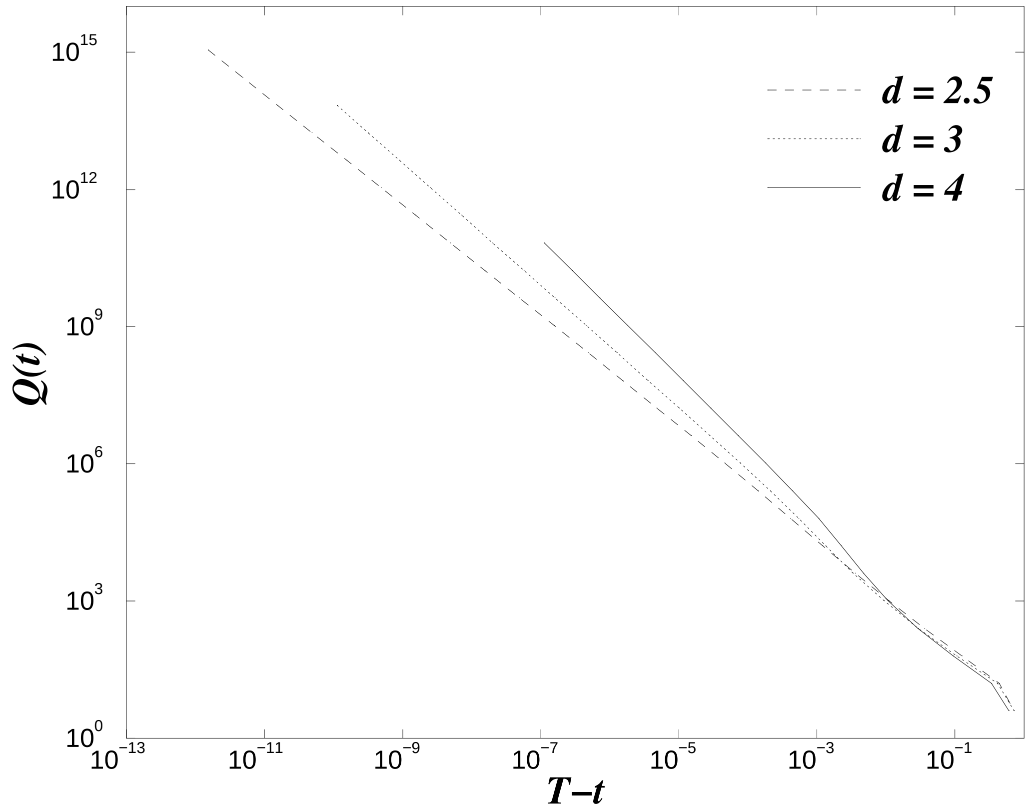

Figure 9. The height $Q(t)$ for $d = 2.5, 3$ and 4. In the asymptotic regime, the best fits have slopes of value 1.203, 1.335 and 1.498 respectively, in good agreement with the theoretically predicted values of 6/5, 4/3 and 3/2.

Generalizing an argument from [14], a simple motivation for the power laws in Eq. (35) goes as follows. We begin by assuming that $\delta \ll R \ll 1$ and that the peak

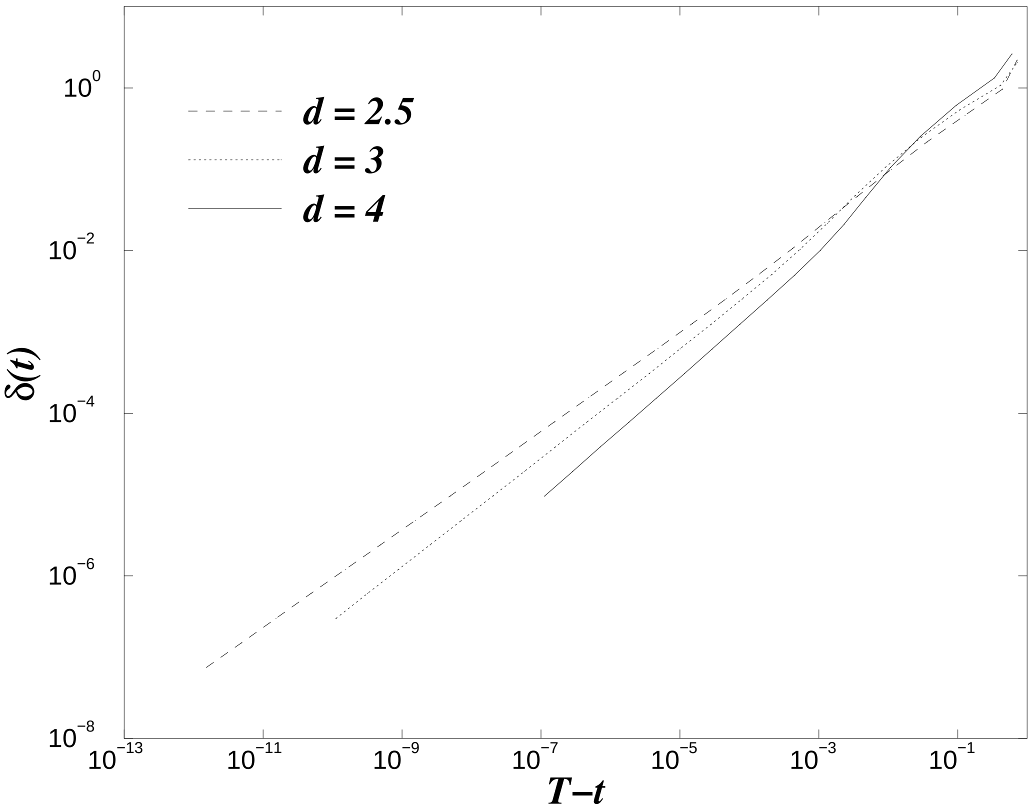

Figure 10. The width $\delta(t)$ for $d = 2.5, 3$ and 4. In the asymptotic regime, the best fits have slopes of value 0.602, 0.668 and 0.749 respectively, in good agreement with the theoretically predicted values of 3/5, 2/3 and 3/4. Here, δ is defined as the width at half the height of the peak.

contains a finite and slowly changing portion of mass, namely that $m(R,t) \sim R^{d-1}h\delta \sim M$. In the neighborhood of the peak, we have $\partial_r\rho \sim h/\delta$ and $\partial_r^2\rho \sim h/\delta^2$, so that the second term in the RHS of Eq. (9) becomes asymptotically irrelevant, leading to

$$\partial_t\rho = \partial_r^2\rho + \frac{1}{r^{d-1}}\partial_r(m\rho). \tag{36}$$

We will require that the three remaining terms to be of the same size. Recalling that $\partial_r m = r^{d-1}\rho$, we obtain

$$h\delta^2 \sim 1. \tag{37}$$

With the mass conservation assumption, this leads to

$$\delta \sim R^{d-1}. \tag{38}$$

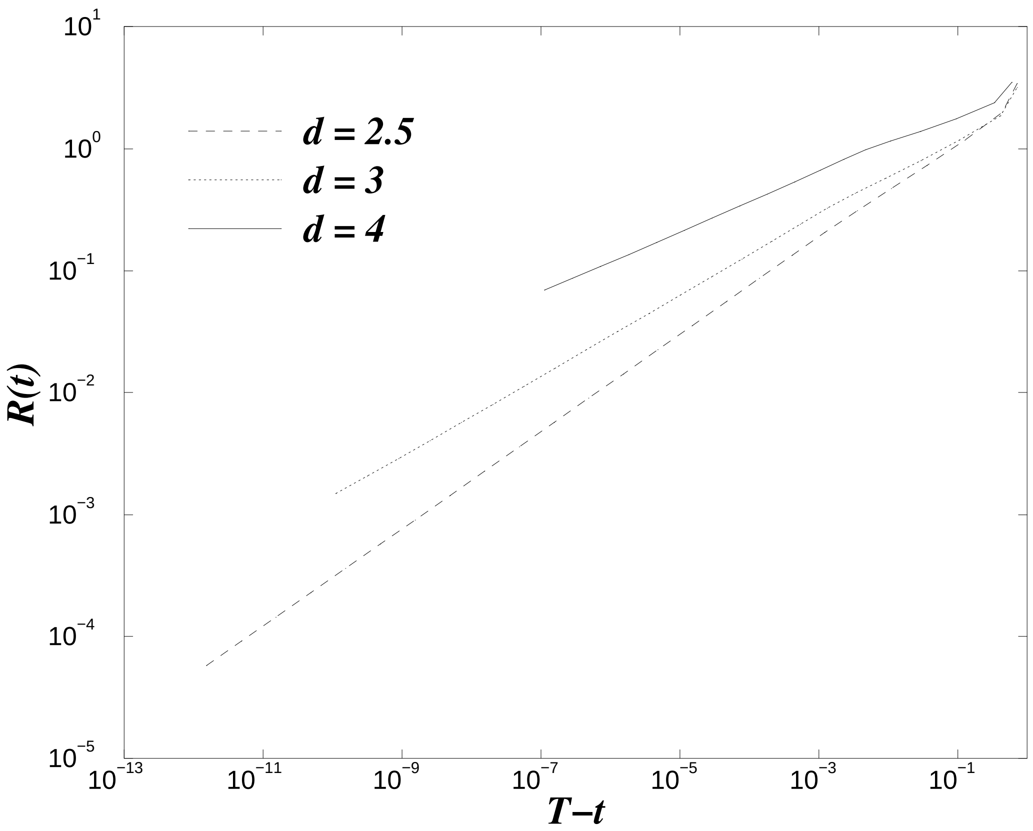

Figure 11. The location $R(t)$ for $d = 2.5, 3$ and 4. In the asymptotic regime, the best fits have slopes of value 0.399, 0.327 and 0.246 respectively, in good agreement with the theoretically predicted values of 2/5, 1/3 and 1/4.

Those relations together with $R \ll 1$ imply for $d > 2$ that (36) is in turn asymptotically equivalent to

$$\partial_t \rho = \partial_r \left(\partial_r \rho + \frac{m}{r^{d-1}} \rho \right). \tag{39}$$

To estimate $R(t)$, we next consider traveling wave solutions of Eq. (39) of the form $\rho(r,t) = \varphi(\xi)$, $\xi = r - R(t)$. Assuming that φ and φ' decrease to zero as $\xi \to \infty$ and integrating the equation for φ once, yields

$$-\dot{R}\varphi = \varphi' + \frac{m}{(\xi + R)^{d-1}} \varphi.$$

At $\xi = 0$ we have $\varphi' = 0$, so that

$$\dot{R} \sim -\frac{M}{R^{d-1}}.$$

This yields the power law for $R(t)$ in Eq. (35). The behaviors of δ and Q follow from Eq. (37) and Eq. (38).

4.3. Asymptotic solutions neglecting diffusion

In the previous section, we discussed solutions that lead to blowup on scales different from the parabolic scaling $\eta = r/\sqrt{T-t}$. In this section, we will discuss the structure solutions that blowup at time T on scales $L(t) \gg \sqrt{T-t}$ with $L(t) \to 0$ as $t \to T$, so that the density blows up at $t = T$ but the diffusion term becomes asymptotically irrelevant. Since the nonlinearity gives $\partial_t \rho \sim \rho^2$, we consider the following *ansatz* for solutions that blow up at $t = T$:

$$\rho(r,t) = \frac{1}{T-t}\Pi(\eta,\tau)$$

where η is the similarity variable $r/L(t)$, $L(t)$ is an as yet unspecified function of t and $\tau = -\log(T-t)$. To describe a blowup we will require that Π satisfy the boundary conditions

$$\Pi(0) < \infty, \quad \Pi(\eta) \to 0 \text{ as } \eta \to \infty,$$

with $\Pi(\eta) \geq 0$ for all $\eta \geq 0$. As before, we shall eventually go to a similarity solution by requiring that the solution be τ independent. Using the above *ansatz*, Eq. (10) gives

$$b(r,t) = \frac{1}{T-t}B(\eta,\tau)$$

and Eq. (12) can be written in the form:

$$\partial_\tau B + B - (T-t)\frac{d\log L}{dt}\eta\partial_\eta B = \frac{T-t}{L^2(t)}\bar{\Delta}_{d+2}B + \frac{B}{d}\eta\partial_\eta B + B^2, \qquad (40)$$

where $\bar{\Delta}_{d+2}$ is the $d+2$ dimensional Laplacian in η. Using $L(t) \gg \sqrt{T-t}$, we see that the diffusive term is asymptotically irrelevant in comparison to the nonlinearity. Assuming that we approach a τ independent solution for B as $\tau \to \infty$, we obtain the asymptotic equation

$$\left[\frac{B}{d} - \alpha\right]\eta\partial_\eta B = B - B^2, \qquad (41)$$

with

$$\alpha = -\lim_{t\to T}(T-t)\frac{d\log L}{dt}.$$

In particular, for $L(t) = (T-t)^\beta$, we have $\alpha = \beta$ and $L(t) \gg \sqrt{T-t}$ requires that $\alpha \geq 1/2$. The case $\alpha = 1/2$ occurs for example with $L(t) = \sqrt{(T-t)|\log(T-t)|}$ which is the scaling for a family of solutions for the semi-linear heat equation [12].

From the boundary conditions specified above, we see that the solution should satisfy

$$B(0) < \infty \quad \text{and} \quad B(\eta) \to 0 \text{ as } \eta \to \infty.$$

Defining $\xi = \log \eta$, Eq. (41) can be written as the autonomous system

$$B_\xi = d\frac{B - B^2}{B - d\alpha}. \tag{42}$$

The fixed point at $B = 0$ is stable, the fixed point at $B = 1$ is repelling, and there are no critical points in the interval $(0, 1)$ if $\alpha > 1/d$. Consequently, for $1/d < \alpha \leq 1/2$, given any $C \in (0, 1)$, we have a solution of Eq. (42) with $B(\xi = 0) = C$,

$$\lim_{\xi \to -\infty} B = 1 \quad \text{and} \quad \lim_{\xi \to \infty} B = 0,$$

so that it satisfies the boundary conditions. We therefore have a continuous family of solutions for each α that satisfy the boundary conditions. We can integrate Eq. (42) to obtain the implicit solutions

$$\left(\frac{1 - B}{B}\right)^\alpha (1 - B)^{-1/d} = ke^\xi = k\eta, \tag{43}$$

where $k \in (0, \infty)$ is an arbitrary constant that parameterizes the continuous family of solutions. These solutions satisfy $B \approx 1 - k_1\eta^{d/(d\alpha - 1)}$ for small η and $B \approx k_2\eta^{-1/\alpha}$ for large η where k_1 and k_2 are constants that depend on the parameter k.

5. Stability and convergence properties of blowup profiles

In Sec. 4.1, we saw that the system has a countable number of possible self-similar blowup profiles with the parabolic scaling (Eq. (27)). This brings up the question of which of these profiles are stable (that are seen if we start from arbitrary initial data).

5.1. Stability of the blowup profiles

We will now prove the following result concerning the stability of the various blowup profiles.

Theorem 5. *Every self-similar solution $H_S(\eta)$ that blows up at a finite time has an unstable mode corresponding to changing the blowup time. Also, a blowup profile with n extrema in $(0, \infty)$ has at least n additional unstable modes.*

Proof. Linearizing Eq. (31) about $H = H_S$, we obtain

$$\begin{aligned}\partial_\tau \Phi(\eta, \tau) = \partial_\eta^2 \Phi(\eta, \tau) &+ \left(\frac{d - 3 + 2H_S(\eta)}{\eta} - \frac{\eta}{2}\right)\partial_\eta \Phi(\eta, \tau)\\ &+ \frac{2\eta\partial_\eta H_S(\eta) + 2(d - 2)(2H_S(\eta) - 1)}{\eta^2}\Phi(\eta, \tau).\end{aligned} \tag{44}$$

We will consider the eigenvalue problem for the above equation. For a given λ, let Φ_λ be a solution of

$$\begin{aligned}&\partial_\eta^2 \Phi_\lambda(\eta) + \left(\frac{d - 3 + 2H_S(\eta, t)}{\eta} - \frac{\eta}{2}\right)\partial_\eta \Phi_\lambda(\eta)\\ &+ \left[\frac{2\eta\partial_\eta H_S(\eta) + 2(d - 2)(2H_S(\eta) - 1)}{\eta^2} + \lambda\right]\Phi_\lambda(\eta) = 0.\end{aligned} \tag{45}$$

Then, $\Phi_\lambda(\eta)e^{-\lambda\tau}$ is a solution of Eq. (44). Near $\eta = 0$, the leading behaviors of the two linearly independent solutions of (45) are $\Phi_\lambda(\eta) \sim \eta^2$ and $\Phi_\lambda(\eta) \sim 1/\eta^{d-2}$. To have H nonsingular near $\eta = 0$, we will require the boundary condition

$$\Phi_\lambda(\eta) \to \eta^2 \text{ as } \eta \to 0.$$

For large η, the leading behaviors of the two independent solutions are $\Phi_\lambda(\eta) \sim \eta^{-(2\lambda+1)}e^{\eta^2/4}$ and $\Phi_\lambda(\eta) \sim \eta^{2\lambda}$. Although the functions $\eta^{2\lambda}$ diverge as $\eta \to \infty$, in terms of r and t, we have

$$\eta^{2\lambda}e^{-\lambda\tau} = r^{2\lambda},$$

is bounded for r bounded as $t \to T$. Consequently, the solutions which behave like $\eta^{2\lambda}$ are admissible but the functions that behave like $\eta^{-(1+2\lambda)}e^{\eta^2/4}$ diverge at finite r as $t \to T$ and are consequently inadmissible. We are interested therefore in finding λ_n so that the solution $\Phi_{\lambda_n}(\eta)$ also satisfies the boundary condition

$$\Phi_{\lambda_n}(\eta)e^{-\eta} \to 0 \text{ as } \eta \to \infty.$$

We have the freedom to choose the blowup time T, *i.e.*, $H_S(r/\sqrt{T+\delta-t})$ is a solution to Eq. (13) for all δ. Using $\eta = r/\sqrt{T-t}$ and $\tau = -\log(T-t)$, we see that, setting $H(\eta,\tau) = H_S(\eta,\tau,\delta)$ yields an identity where

$$\bar{H}_S(\eta,\tau,\delta) = H_S(r/\sqrt{T+\delta-t}) = H_S\left(\eta\sqrt{\frac{e^{-\tau}}{e^{-\tau}+\delta}}\right)$$

Differentiating the resulting identity *w.r.t.* δ, setting $\delta = 0$, and comparing the resulting equation with Eq. (45), we see that $F_S^0(\eta) = \eta\partial_\eta H_S(\eta)$ is an eigenfunction with an eigenvalue $\lambda = -1$ since it also satisfies the boundary conditions $F_S^0(\eta) \sim \eta^2$ as $\eta \to 0$ and $F_S^0(\eta)e^{-\eta} \to 0$ as $\eta \to \infty$. If the function $H_S(\eta)$ has k extrema in $(0,\infty)$, the function $\Phi_{-1}(\eta) = F_S^0(\eta)$ has k zeroes in $(0,\infty)$. Now, by standard results from Sturm-Liouville theory, it follows that there exist $\lambda^*_{-k} < \ldots < \lambda^*_{-2} < \lambda^*_{-1} < \lambda^*_0 = -1$ such that $\Phi_{\lambda^*_{-j}}(\eta)e^{-\eta} \to 0$ as $\eta \to \infty$ and $\Phi_{\lambda^*_{-k}}(\eta)$ has exactly $k-j$ zeroes in $(0,R)$.

The eigenfunctions with eigenvalues less than zero are unstable. This proves our claim that all the self-similar blowup profiles $H_S(\eta)$ have an unstable mode corresponding to changing the blowup time. Further, a blowup profile with k extrema in $(0,\infty)$ has at least k additional unstable modes. □

This theorem implies that a self-similar blowup profile that is stable to small perturbations in the initial conditions (except for possibly a change in the blowup time) cannot have any extrema for $\eta \in (0,\infty)$.

5.2. Convergence to the stable blowup profile

A formal procedure for determining the stability of blowup profiles is as follows. We will assume that we are sufficiently close to the blowup so that we can use the linear equation (44) to describe the stability of the blowup profile $H_S(\eta)$. If we choose the blowup time

T correctly in the definition of τ and η, we can eliminate the mode corresponding to the change in blowup time. From the linear analysis in the preceding section, we have

$$H(\eta,\tau) = H_S(\eta) + aF_S^1(\eta)e^{-\lambda_1\tau} + O(e^{-\lambda_2\tau}), \tag{46}$$

close to the blowup, where λ_1 and λ_2 are respectively the smallest and the next to smallest eigenvalues in the set of all the eigenvalues of the Eq. (45) excluding the eigenvalue -1. F_S^1 is the eigenfunction corresponding to λ_1 and a is an constant depending on the initial conditions, generically not equal to zero.

If the blowup profile is stable to small perturbations in the initial conditions, it follows from Eq. (46) that

$$\lambda_1 > 0.$$

Given a similarity solution H_S, we can calculate λ_1 numerically from Eq. (44). For $d = 3$ and $H_S(\eta) = H_0(\eta) = 2\eta^2/(2(d-2)+\eta^2)$, we obtain $\lambda_1 \approx 0.27$. We also find that $\lambda_1 > 0$ for $H_0(\eta)$ for all $d > 2$. Therefore, the similarity solution

$$H_0(\eta) = \frac{2\eta^2}{2(d-2)+\eta^2},$$

will be seen generically in solutions that blow up according to the parabolic scaling. Using $h(r,t) = H(\eta,\tau)$ and the definition of h, we get

$$\begin{aligned}\rho(r,t) = {} & \frac{4(d-2)(2d(T-t)+r^2)}{(r^2+2(d-2)(T-t))^2} + a\frac{(T-t)^{\lambda_1}}{T-t}\Pi_1^1\left(\frac{r}{\sqrt{T-t}}\right) \\ & + O((T-t)^{\lambda_2-1}),\end{aligned} \tag{47}$$

where

$$\Pi_1^1(\eta) = \frac{1}{\eta^{d-1}}\partial_\eta(2\eta^{d-2}F_1^1(\eta)).$$

Using the fact $F_1^1(\eta) \to \eta^2$ as $\eta \to 0$, we have

$$\rho(0,t) = \frac{1}{(T-t)}\left[\frac{2d}{d-2} + 2ad(T-t)^{\lambda_1} + o((T-t)^{\lambda_2})\right]. \tag{48}$$

For $d = 3$, this formal procedure yields the prediction

$$\rho(0,t) \approx \frac{6}{T-t}\left[1 + C(T-t)^{0.27}\right].$$

where the constant C is generically not equal to zero. Fig. 12 is a plot generated by numerically solving the system in Eq. (1) and it agrees well with this prediction.

In Sec. 4.1, we saw that there exist two solutions to Eq. (32) each having one intersection with the line $H = 1$ and no extrema for $\eta \in (0,\infty)$. In the above discussion we showed that the solution in (33) gives a stable self-similar profile. Numerically calculating λ_1 and λ_2 for the solution $H_*(\eta)$ in $d = 3$, we see that $\lambda_1 \approx -0.443 < 0$ and $\lambda_2 > 0$. Therefore, although the solution $H_*(\eta)$ has no extrema for $\eta \in (0,\infty)$, it has one unstable mode (besides the mode that changes the blowup time). This explains why we do not see blowup corresponding to the solution $H_*(\eta)$ in numerical simulations with arbitrarily chosen initial data. Numerically calculating the eigenvalues for the

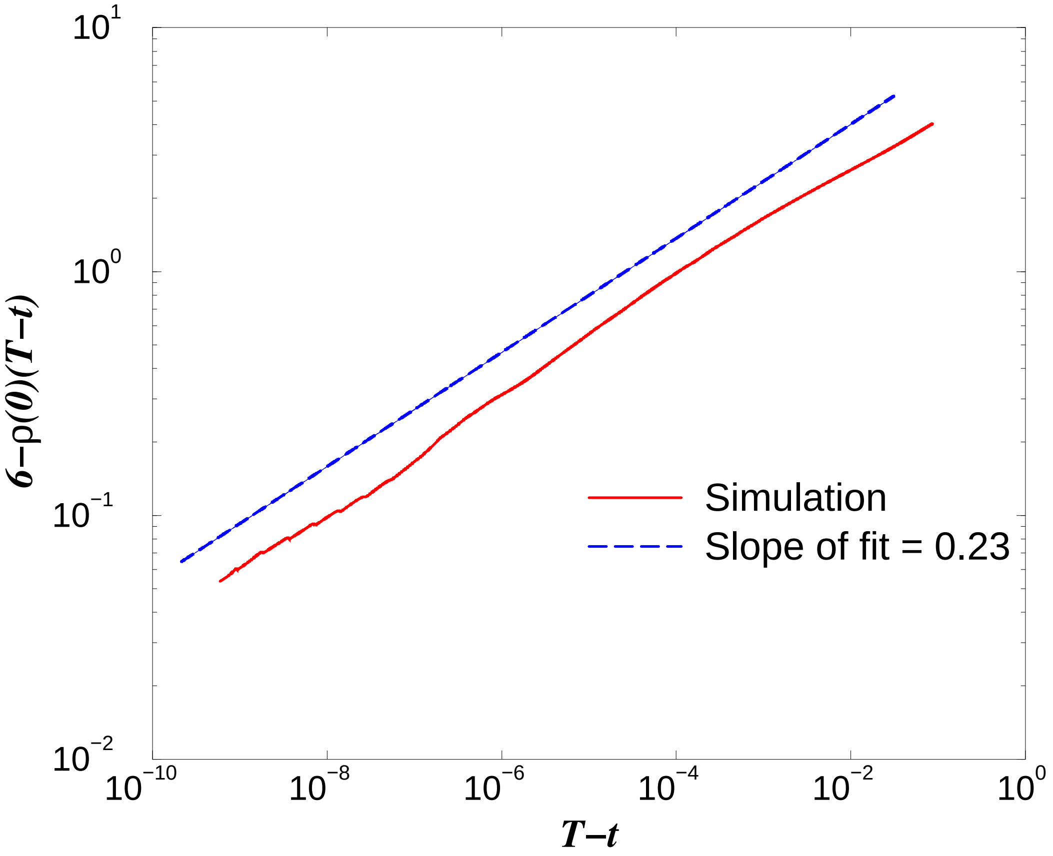

Figure 12. Convergence to the Blowup profile. The slope of the best fit is 0.23 in good agreement with the linear analysis which gives 0.27. Note that this exponent is small so that the convergence is very slow and one has to solve the equations until very close to the blowup time to see the convergence to the self-similar solution.

linearization about the solution H_1 gives $\lambda_1 \approx -77.2$ and $\lambda_2 > 0$, so that the blowup profile given by H_1 also has one linearly unstable mode besides the mode that changes the blowup time.

6. The Phase Portrait for the system

6.1. Critical solutions

The analysis in the previous sections has led us to the identification of several stable final states for the solutions of the system in (1) with spherical symmetry. For $d > 2$ and on bounded domains, we see that there exist open sets of initial conditions for which the system can :

(i) Converge to a stable steady state given by $h_0(r)$ as $t \to \infty$ (see Sec. 3.1),

(ii) Blow up at a finite time T converging to the self-similar blowup profile given by $H_0(\eta)$ in Eq. (33) (see Sec. 4.1), or

(iii) Blow up at a finite time T in a non self-similar fashion (see Sec. 4.2 and Eq. (35)).

The fate of an initial condition depends not only on its conserved total mass, but also on the density distribution $\rho_0(r)$. The existence of more than one kind of stable behavior brings up the question of what determines the boundaries (separatrices) between the different sets of initial conditions that correspond to different final states. A related question is what happens to solutions whose initial data lies on the separatrix between the basins of attraction of two different types of stable behaviors.

We investigate these questions numerically by following the solutions for a family of initial conditions $\rho_0(r, p)$ parameterized by a parameter p. The family of initial conditions is chosen such that the final states for the initial conditions given by $p = p_0$ and $p = p_1$ are different. In that case, there exists at least one critical value $p_c \in (p_0, p_1)$ such that the final states for initial conditions for any p_a and p_b sufficiently close to p_c with $p_a < p_c < p_b$ are different. We find the critical value p_c by successive bisection and we can determine the separatrix by following the solution with initial condition $\rho_0(r, p_c)$ for different families of initial conditions.

Using this bisection method, we investigate the separatrices between the initial conditions that converge to the steady solution h_0, that blowup in a self-similar fashion given by H_0, and that blowup in a non self-similar manner by an imploding shock. We find that the boundaries between initial conditions leading to different kinds of stable behavior are sets of initial conditions that "converge" to "unstable behaviors" with one unstable direction (codimension one asymptotic behaviors). If the relevant unstable behavior is a steady state with one unstable direction, then both ρ or h converge uniformly on compact sets to the appropriate limits. On the other hand, it is also possible that the relevant behavior is a blowup modality that has an unstable mode besides the mode that changes the blowup time. In this case, the rescaled density $\Pi(\eta, \tau)$ and $H(\eta, \tau)$ converge uniformly to the appropriate limits on compact sets in the similarity variable η as $\tau \to \infty$.

We will refer to the final states for initial conditions lying on the separatrix between different basins of attraction as critical solutions. If we choose an initial condition $\rho_0(r, p_d)$ with p_d close to the critical value p_c, the solution has a transient phase when it stays close to the separatrix and seems to converge to the critical solution. However, it will eventually move away from the critical solution along the unstable direction and end up in one of the stable final states for the system.

For $2 < d < 10$, if the total mass is smaller than the critical mass $M_c(R)$ for a domain of size R (See Eq. (20)), one possible final state is the stable steady state given by $h_0(r)$. Numerical evidence suggests that the separatrix $\mathcal{M}_0$ between the stable steady state and the stable self-similar blowup contains at least two pieces. One piece $\mathcal{M}_a$ is given the initial conditions that converge to the steady state $h_1(r)$ that has one unstable mode. Another piece $\mathcal{M}_b$ is given by the set of solutions converging to the self-similar blowup profile given by $H_1(\eta)$, which also has one unstable direction (if we eliminate the mode that changes the blowup time).

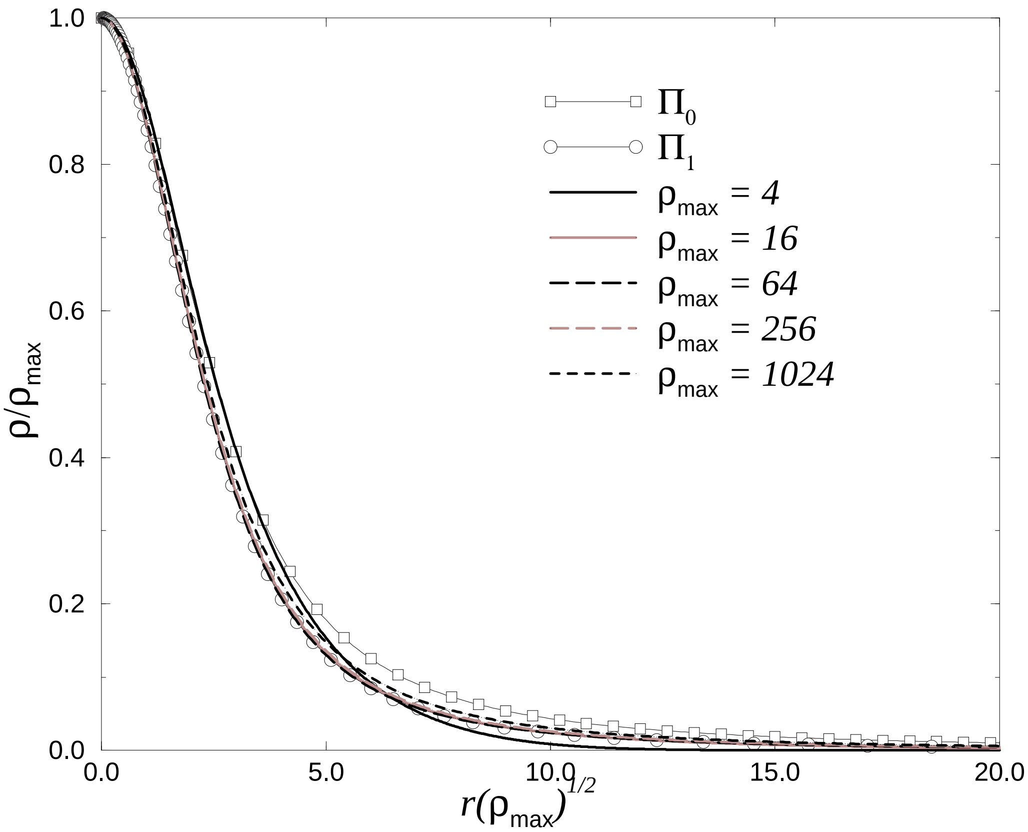

Figure 13. Rescaled solutions in $d = 3$ for an initial condition that is close to the separatrix between solutions converging to the steady state and self-similar blowup with a profile given by H_0 (Stable blowup). In this case, the relevant critical solution is the self-similar blowup given by H_1.

Figure 13 shows numerically obtained solutions of Eq. (9) in $d = 3$ for an initial condition that is very close to the separatrix between between solutions converging to the steady state and self-similar blowup with a profile given by H_0 (Stable blowup). In this case, the relevant critical solution is the self-similar blowup given by H_1. A linearization about this solution gives an unstable eigenvalue $\lambda \approx -77.2$. Since this is very large, it is difficult to obtain solutions with a long transient phase during which the solution is close to the critical solution H_1. In this case, it is also difficult to estimate the blowup time appropriate for the solution in the transient phase since there are solutions close to the critical solution that converge to the stable steady state and hence are global in time. Therefore, we normalize the density, using it's maximum value ρ_{max}, rather than the inverse of the time to blowup $1/(T-t)$ and the radial co-ordinate by $\rho_{max}^{-1/2}$ rather that $\sqrt{T-t}$. This implies that we have effectively used one-fitting parameter to obtain the agreement of the curves in Fig. 13.

We also investigate the separatrix between the basins of the self-similar blowup and non self-similar blowup. In this case, the relevant critical solution turns out to be the blowup modality H_*. Our solutions follow track this blowup profile until very close to the time of blowup. They eventually diverge away from the critical solution but during this transient period, the density blows up on the self-similar scales and converges in the similarity variables towards a profile which is in very good agreement with the solution Π_* corresponding to the unstable solution H_*.

Figure 14 shows numerically obtained solutions of Eq. (9) in $d=3$ for an initial condition that is very close to the separatrix between the self-similar blowup and non self similar blowup. Since the unstable eigenvalue corresponding to H_*, $\lambda \approx -0.443$ is not very large, it is possible to find initial conditions such that the solutions remain close to the critical solution during the interval where ρ_{max} grows by many orders of magnitude. Also, in this case, it is possible to estimate the blowup time relevant to the transient regime by setting it equal to the blowup time of the solution. Although the solution will move away from the critical solution and blowup, and toward one of the stable blowup modes, the errors we make are very small since the solution stays close to the critical solution until about 10^{-22} before the blowup. The density is normalized by the inverse of the time to blowup and the radial coordinate is scaled by the square root of the time to blowup. The function Π_* is also shown for comparison. Note that the scaled density profiles eventually start to diverge away from the curve given by Π_* (for $t \sim T - 10^{-22}$).

6.2. Connections and the global phase portrait

We will first consider the case of solutions on a bounded domain B_R. From the analysis of the structure and the stability of the various solutions, we see that there is a correspondence between the blowup modality H_k and the steady solution h_k. They both have k extrema and k linearly unstable modes. The solution H_* has one linearly unstable mode and the solution S (the Burger-like shock) is stable. Based on the numerical results that we discuss in the preceding section, we make the following conjectures about the structure of the phase space for radial solutions on a bounded domain:

(i) The steady solution h_k and the blowup modality H_k each has connections with the $2k$ behaviors $\{h_i, H_i\}, i = 0, 1, \ldots, k-1$.

(ii) The behavior H_* has connections with the stable self-similar blowup H_0 and the Burger-like shock S.

Figure 4 illustrates some of these conjectures.

For the case of the unbounded domain, we no longer have the multiple steady solutions $h_0, h_1, \ldots$. Instead, we have a family of self-similar decaying solutions given

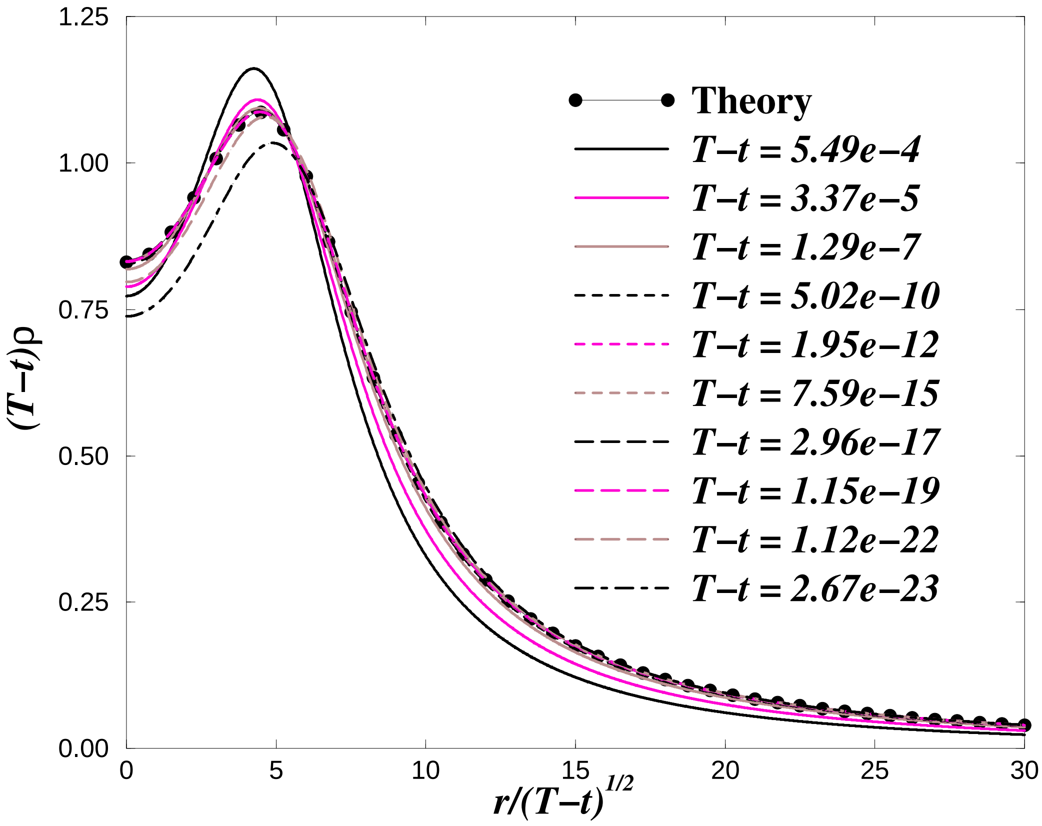

Figure 14. Blowup profile in $d = 3$ for an initial condition that is close to the separatrix between the self-similar blowup and the non self-similar blowup. The blowup time T is the blowup time for the solution. T is very close to the blowup time of the unstable solution that it tracks in the transient phase because the initial condition is chosen very close to the separatrix. The theoretical curve is the density profile for the solution Π_* and there are no parameters that are fit.

by $h(r,t) = \bar{H}(r/\sqrt{t})$. These solutions converge to $h(r) = 0$ uniformly on compact sets. The number of these solutions is a function of ν defined by

$$\nu = \lim_{r\to\infty} h(r,t) = \lim_{\zeta\to\infty} \bar{H}(\zeta),$$

and there exist $N = \bar{N}(\nu)$ self-similar decaying solutions given by the profiles $\bar{H}_0(\zeta), \bar{H}_1(\zeta), \ldots, \bar{H}_{N-1}(\zeta)$, with $\lim_{\zeta\to\infty} \bar{H}_k(\zeta) = \nu$ for all k. The transient solution $h(r,t) = \bar{H}_k(r/\sqrt{t})$ has k extrema in $(0,\infty)$ and it has k linearly unstable directions [35], so that it is analogous to the solution h_k on a bounded domain. Our conjectures for the structure of the phase space for solutions on unbounded domains are:

(i) The behaviors H_k and $\bar{H}_k$ have connections with the $2k$ behaviors $\{H_i, \bar{H}_i\}, i =$

$0, 1, \ldots, k-1$.

(ii) The behavior H_* has connections with the blowup modality H_0 and the Burger-like shock S.

7. Conclusions

We study a parabolic-elliptic system (1) which describes the evolution of a compressible active scalar that diffuses and is advected by the gradient it generates. We have discussed the existence, stability and connections between steady solutions, parabolic self-similar blowup solutions and Burgers like blowup solutions for this system. We find that the system has rich dynamics with multiple steady states, multiple parabolic self-similar blowups and non self-similar blowup. We prove results on the number of linearly unstable modes for the various steady solutions and the self-similar blowup profiles. Numerically, we find heteroclinic connections between different modalities of blowup, between steady states and blowup, and most remarkably between blowup and steady states. Using these connections and the correspondence between the number of unstable directions of the various solutions, we begin to sketch a global phase portrait that encompasses both the smooth behavior and the singularity formation. This task is not completed yet and we expect the situation to be rather complicated. There remain many open problems, among them the connections between the unstable steady states and the unstable self-similar blowup profiles; the role of the solutions from Sec. 4.3 that are not self-similar with the parabolic scaling; questions about the similarities and the differences between the phase portraits for finite domains and for unbounded domains; and last but not the least, proving the conjectures about the structure of the phase space.

Acknowledgments

We wish to thank Frank Merle for valuable discussions. We also wish to thank Bruce Ayati, Howard Berg, Elena Budrene, Todd Dupont, Leonid Levitov and Saleh Tanveer for many useful discussions. The work of A.S. was supported by the Fonds National Suisse. The work of M.B. was supported by the National Science Foundation (Department of Mathematical Sciences). The work of P.C., L.P.K and S.C.V. was supported by the MRSEC program of the National Science Foundation under Award Number DMR-9808595. L.P.K was also supported by the ONR grant N00014-96-1-0127 and the NSF gran DMR 9728858.

[1] Keller E F and Segel L A 1970 *J. Theor. Biol.* **26** 399–415;
Murray J 1989 *Mathematical Biology* (Berlin: Springer–Verlag)

[2] S Chandrasekhar 1967 *An introduction to the study of stellar structure* (New York: Dover)

[3] Wolansky G 1992 *Arch, Rat. Mech. Anal.* **119** 355-391;
Wolansky G 1992 *J. Analyse Math.* **59** 251-272

[4] Biler P and Nadzieja T 1994 *Colloquium Mathematicum* **LXVI** 319–334

[5] Evans C R and Coleman J S 1994 *Phys. Rev. Lett.* **72** 1782–1785;
Koike T, Hara T and Adachi S 1995 *Phys. Rev. Lett.* **74** 5170–5173;

Gundlach C 1997 *Phys. Rev. D* **55** 695–713;
Bizon P 1996 `http://xxx.lanl.gov/abs/gr-qc/9606060`
[6] Budrene E O and Berg H C 1991 *Nature* **349** 630 ;
Budrene E O and Berg H C 1995 *Nature* **376** 49–53
[7] Brenner M P, Levitov L and Budrene E O 1998 *Biophys. J.* **74** 1677
[8] Barenblatt G I 1979 *Similarity, Self Similarity and Intermediate Asymptotics* (New York: Consultants Bureau)
[9] Landman M J *et al* 1988 *Phys. Rev. A* **38** 3837;
V. M. Malkin 1993 *Physica D* **64** 251;
D. W. McLaughlin *et al* 1986 *Phys. Rev. A* **34** 1200;
G.G. Luther, A.C. Newell and J. V. Maloney 1994 *Physica D* **74** 59;
G. M. Fraiman 1985 *Sov. Phys. JETP* **61** 228
[10] Giga Y and Kohn R V 1985 *Comm. Pure Appl. Math.* **38** 297–319
[11] Herrero M A and Velázquez J J L 1996 *Math. Ann.* **306** 583–623
[12] Bricmont J and Kupiainen A 1994 *Nonlinearity* **7** 539–575
[13] Merle F and Zaag H 1998 *Comm. Pure Appl. Math.* **51** 139–196
[14] Herrero M A, Medina E and Velázquez J J L 1997 *Nonlinearity* **10** 1739–1754
[15] Nanjudiah V 1973 *J. Theor. Biol.* **42** 63–105
[16] Childress S and Percus J 1981 *Math. Biosci.* **56** 217–237
[17] Jäger W and Luckhaus S 1992 *Trans. Am. Math. Soc.* **329** 819–824
[18] Biler P, Hilhorst D and Nadzieja T 1994 *Colloquium Mathematicum* **LXVII** 297–308
[19] Biler P 1995 *Studia Mathematica* **114 (2)** 181–205
[20] Nagai T 1995 *Adv. Math. Sci. Appl.* **5** 581–601
[21] Diaz J I and Nagai T 1995 *Adv. Math. Sci. Appl.* **5** 659–680
[22] Herrero M A and Velázquez J J L 1996 *Math. Ann.* **306** 583–623
[23] Herrero M A, Medina E and Velázquez J J L 1997 Self-Similar Blow-Up for a Reaction-Diffusion system *preprint*
[24] Gajewski H and Zacharias K 1998 *Math. Nachr.* **195** 77–114
[25] Biler P and Nadzieja T 1998 *Adv. Diff. Eqs.* **3** 177–197
[26] Biler P 1998 *Adv. Math. Sci. Appl.* **8** 715–743
[27] Babin A V and Vishik M I 1992 *Attractors of Evolution Equations* (Amsterdam: North Holland)
[28] Temam R 1988 *Infinite-Dimensional Dynamical Systems in Mechanics and Physics* (New York: Springer-Verlag)
[29] Samarskii A A, Galaktionov V A, Kurdyumov S P and Mikhailov A P 1995 *Blow-up in Quasilinear Parabolic Equations* (Berlin: Walter de Gruyter)
[30] Ayati B P 1996 *BuGS 1.0 User Guide*, Technical Report TR–96–18, Department of Computer Science, University of Chicago
[31] Protter M H and Weinberger H F 1967 *Maximum Principles in Differential Equations* (Engelwood Cliffs: Prentice–Hall)
[32] Evans L C and Gariepy R F 1992 *Measure Theory and Fine Properties of Functions* (Boca Raton: CRC Press)
[33] Biler P and Woyczyński W A 1997 Global and Exploding Solutions For Nonlocal quadratic Evolution Problems *preprint*
[34] Brenner M P, Constantin P, Kadanoff L P, Schenkel A and Venkataramani S C 1998, Technical Report, `http://mrsec.uchicago.edu/~scvenkat/pubs/singular.ps`
[35] Constantin P, Merle F and Venkataramani S C *in preparation*